

Research Papers

Impact of demand response on battery energy storage degradation using gbest-guided artificial bee colony algorithm with forecasted solar insolation



Dipanshu Naware^{a,*}, Raviteja Badigenchala^a, Arghya Mitra^a, Debapriya Das^b

^a Department of Electrical Engineering, Visvesvaraya National Institute of Technology, Nagpur, M.S. 440010, India

^b Department of Electrical Engineering, Indian Institute of Technology, Kharagpur, W.B. 721302, India

ARTICLE INFO

Keywords:

Autoencoder
Battery degradation
Cycelife
Demand response
GABC
LSTM

ABSTRACT

The role of energy storage technology is gaining momentum as prosumers are actively participating in the retail electricity market. For the local energy community equipped with a grid-tied rooftop photovoltaic (PV) system, battery energy storage (BES) is a vital element to overcome the reliability issues occurring due to intermittency in renewable energy sources (RES). The PV-BES combination at the residential level is quite challenging as it involves optimal sizing and economical operation of the system. Also, rechargeable batteries are prone to aging and are majorly affected by temperature, state-of-charge (SOC), and charge/discharge rates (C_{rate}), resulting in degradation and shortened useful life of BES. To this end, a single-objective optimization for minimizing the total degradation cost of BES is presented. In the first phase of this work, the day-ahead solar insolation is forecasted with an outlier filter-based autoencoder long short-term memory (LSTM-AE) for enhanced prediction accuracy. The mean absolute error (MAE), mean bias error (MBE), and coefficient of determination (R) of the LSTM-AE model are found to be 0.0423, -0.0117, and 0.984 respectively. The emergency demand response program (EDRP) is modeled in the second phase. An incentive of 20 €/kWh is found to balance the service provider (SP) revenue and prosumer benefit (PB) for prosumer participation in EDRP. Furthermore, the degradation cost of BES with an initial status of 20%, 55%, and 95% of SOC is optimized using a tuned gbest-guided artificial bee colony (GABC) algorithm both in the absence and presence of EDRP. The optimal solution obtained with EDRP shows daily savings, with three initial status of SOC, to be 18.78%, 12.14%, and 11.18% for summer, 16.15%, 13.77%, and 8.88% for mild, and 20%, 15.65%, and 12.16% for winter respectively, when compared without EDRP. Hence, this study demonstrates the merits of planning and prosumer participation in the retail electricity market and has a potential application in the real local energy community. The grid-connected PV-BES residential system is implemented in Python-Jupyter Notebook and MATLAB.

1. Introduction

With the continuous depletion of fossil fuels and the ever-increasing environmental concern, the role of RES in the modern-day microgrid is substantially increasing [1]. Solar, wind, and bio-generation have gained outstanding interest in recent years where the contribution of solar and wind alone accounts for two-thirds of renewables [2]. Due to the intermittent nature of these sources, energy storage units are

actively reformed to address the reliability issues of the system.

Nowadays, a grid-connected rooftop PV along with BES at the residential level is gaining popularity. Prior knowledge of solar PV generation and load demand will help to choose the appropriate size of BES for local energy management. Also based on the daily routine/behavior of residential prosumers, the charging/discharging of BES can be studied. With the integration of rooftop solar PV along with BES, the economic operation of the system becomes extremely challenging, as prior knowledge of energy demand and generation is needed. Hence

Abbreviations: ABC, Artificial bee colony; AE, Autoencoder; BES, Battery energy storage; CNN, Convolutional neural network; DERs, Distributed energy resources; DRP, Demand response program; EDRP, Emergency demand response program; EVs, Electric vehicles; EOL, End of life; GA, Genetic algorithm; GABC, Gbest-guided artificial bee colony; GWO, Grey wolf optimizer; LSTM-AE, Autoencoder long short-term memory; MAE, Mean absolute error; MBE, Mean bias error; MILP, Mixed-integer linear programming; MINLP, Mixed-integer nonlinear programming; OCSVM, One-class support vector machine; PB, Prosumer benefit; PV, Photovoltaic; PJM, Pennsylvania, New Jersey, and Maryland; PMP, Pontryagin's minimum principle; PSO, Particle swarm optimization; R, Coefficient of determination; RES, Renewable energy sources; SOC, State-of-charge; SP, Service provider; TLBO, Teaching-learning based optimization.

* Corresponding author.

E-mail address: dipanshunaware@students.vnit.ac.in (D. Naware).

Nomenclature		Variables and constants
<i>Parameters</i>		
Ah_{nom}	Nominal ampere-hour throughput	Ah_{cyc} Cyclic ampere-hour throughput
C_{bat}	BES initial cost, €/kWh	Ah_{eff} Effective ampere-hour throughput
E_a	Activation energy, J/mol	C_{bd} BES degradation cost, €/kWh
$P_{bat}^{min}, P_{bat}^{max}$	BES minimum and maximum power W	C_{rate} BES Charge/discharge rate
N_p	Population size	C_{edrp} Cost paid to prosumer for EDRP participation, €
S_{1-7}	EDRP scenarios, €/kWh	E_{red} Energy reduction, kWh
soc_{min}, soc_{max}	Minimum and maximum SOC	I_{bat} BES current, A
soc_{nom}	Nominal SOC	P_{pv} Solar PV generation, W
α, β	Fitting coefficients	P_{ch}, P_{dch} BES charging and discharging power, W
η	Compensation factor	P_{load} Prosumers load demand, W
z	Power-law factor	P_{grid} Utility grid power, W
ν	OCSVM Contamination	P_{ini}, P Day-ahead and real-time electricity price, €/kWh
γ	OCSVM kernel coefficient	$Q_{rem}, Q_{surplus}$ BES remaining and surplus capacity, kWh
Q_{loss}	BES Capacity fade %	Q_{avail}, Q_{def} BES available and deficit capacity, kWh
Q_{rated}	BES rated capacity, kWh	soc_{ini} Initial SOC
m, n	EDRP periods	σ Severity factor
θ, λ	Prosumer dependent parameters	φ Discomfort cost to prosumer, €
E	Price elasticity	C Non-negative constant
R	Gas constant	D Decision variable
Δt	Time-step	I, Pen Incentive and penalty, €/kWh

researchers and academicians are investigating various aspects related to this task.

1.1. Related literature

Precise planning study leads to the smooth operation of the system and forecasting has a huge role in power systems. An individual household level energy forecasting is reported in [3] where the combined features of LSTM and convolutional neural network (CNN) are utilized for elevating the forecasting model accuracy whereas for building level, CNN outperforms LSTM, shallow artificial neural networks, factored restricted Boltzmann machines, and support vector machines in [4]. Similarly, for smooth energy management, a deep learning forecaster for PV power prediction is reported in [5] using LSTM-AE whereas a neural network-based intelligent forecast engine is developed in [6] for the prediction of wind power and a similar approach for the prediction of battery, solar and wind power is proposed in [7]. In addition, authors in [8] propose a combined day-ahead forecasting model for the prediction of load and solar insolation with residential prosumers based on the concept of weather classification using LSTM neural networks. Here, the cloud cover plays a vital role in defining prediction accuracy. The time-series data of solar insolation and weather variables are filled with inherent noise elements and there is a possibility of corrupted measurement/false data logging as well. However, the studies conducted in the aforementioned literature [3–7] failed to consider the impact of these anomalies which may deteriorate the forecasting model accuracy to some extent. To address these shortcomings, an LSTM-AE, having an inherent noise removal feature, combined with an outlier filter is proposed in this study for day-ahead solar insolation forecasting.

To address the fluctuations arising due to the exchange of energy with the utility grid, cost-effective storage options, available in the market, play a decisive role by ensuring reliable, uninterrupted, and efficient power supply. BES is proving to be fruitful in concealing fluctuations arising due to small as well as large-scale perturbations in the decentralized environment. Moreover, they can be used to address critical demand under outage scenarios making the system resilient. Major research that revolves around BES, includes load frequency control [9–10], optimal placement and sizing [11–13], degradation analysis

Table 1
Meta-heuristic algorithms in the literature.

Algorithms	Inspiration	Year	Proposer	References
Particle Swarm Optimization	Bird Flock	1995	Kennedy and Eberhart	[23]
Genetic Algorithm	Genetics	1957	AS Fraser	[24–25]
Artificial Bee Colony	Honey Bee	2005	Karaboga	[26]
Grey Wolf Optimizer	Grey Wolves	2013	Seyedali Mirjalili et al.	[27]
Teaching Learning Based Optimization	Classroom	2011	Rao et al.	[28]
Firefly	Firefly	2008	Yang et al.	[29]
Cuckoo Search	Cuckoo	2009	Yang and Deb	[30]
Whale Optimization	Blue Whale	2016	Seyedali Mirjalili et al.	[31]
Marine Predator Algorithm	Ocean Predators	2020	Afshin Faramarzi et al.	[32]

[14–15], lifetime estimation [16–17], voltage fluctuation mitigation [18], and residential peak demand shaving [19]. Authors in [20–22] extensively review the degradation mechanism of lithium-ion BES. The work reported in [14–17] addresses the BES aging performance comprehensively but has few limitations such as the collective impact of C_{rate} , SOC, and ambient temperature on BES degradation, the influence of seasonal variation, and different initial states of the BES. These factors play a huge role in a real-world scenario and hence must be taken into consideration as the optimal operation of the BES system is a significant concern to deal with. On the other hand, optimization methods have always played a vital role in the field of the electricity market for evaluating the optimal solutions and can be classified as deterministic, stochastic, and hybrid techniques. Most of the evolutionary algorithms are stochastic and nature-inspired meta-heuristic techniques. A few of them are listed in Table 1. Particle swarm optimization (PSO) [23], genetic algorithm (GA) [24–25], artificial bee colony (ABC) [26], grey wolf optimizer (GWO) [27], teaching-learning based optimization (TLBO) [28], firefly [29], cuckoo search [30], whale optimization [31], and marine predator [32] are some of the frequently and best-suited algorithms in the context of smart grid as reported below.

For an optimal dispatch of power in a grid-connected PV-BES system,

the degradation cost of the BES is minimized using PSO [33]. The cost optimization of a charging station based on solar PV-BES is achieved using PSO in [34] while the prerequisite knowledge of energy demand and generation is accomplished with the help of neural networks. A hybrid meta-heuristic algorithm combining the features of sine-cosine and crow search algorithm is reported in [35] for solving multi-objective optimization by minimizing the total installation, operation, maintenance, and emission costs, to achieve a robust design of an islanded microgrid with hybrid integration of PV, wind, BES, and electric vehicles (EVs). The optimal sizing of hybrid renewable energy system in the presence of EVs is proposed in [36] with power sharing capabilities. Whale optimization algorithm for optimal placement and sizing is used in [37] with an aim of power loss reduction whereas to enhance the damping in power systems, a mixed-PSO is used for optimal placement and selection of optimal control parameters in [38]. Similarly, for the integration of BES with the distribution networks, a modified African Buffalo Optimization is used [39]. Since its inception in 2005, ABC has gained popularity in solving numerical function optimization. In the field of microgrid, the overall cost of operation along with emission cost is minimized in [40] whereas, for economic dispatch between generation, storage, and load, a multi-period ABC optimization is implemented in [41]. However, to improve the exploitation feature of ABC and to create a good balance between exploration and exploitation, GABC was introduced in 2010 [42]. Since then, GABC has found its application in the microgrid. The optimal integration of distributed energy resources (DERs) incorporated with EVs is achieved using GABC in [43] for improvement in power loss, cost, and emission reduction in the presence of load uncertainty. Similarly, optimal scheduling of energy in a stand-alone microgrid is dealt with in [44] using GABC. Moreover, to study the impact of EVs and wind uncertainty on transmission network planning in the presence of a demand response program (DRP), GABC is used to minimize the total system cost [45].

With the extensive research in the direction of BES development, various aging models were proposed to focus on the capacity fade phenomenon. Authors in [46] establish an aging model for a graphite-lithium ion phosphate BES to study the dependency of C_{rate} on the capacity fade. The useful life of lithium-ion BES is determined in [47–48] using an ampere-hour throughput model, and the impacts of temperature, SOC, and C_{rate} are graphically studied through severity factor mapping. Here, an optimal control strategy for effective energy management is achieved via Pontryagin's minimum principle (PMP) algorithm. A similar coordinated optimal approach is carried out in [49] for minimizing the fuel cost, electricity cost, and BES degradation cost of plug-in hybrid electric buses using the PMP algorithm. Moreover, a multi-objective framework is established in [50] by optimizing the operating cost and energy-saving on a residential PV system considering the impact of BES degradation whereas the total scheduling cost of a microgrid is minimized in [51] by choosing an optimal size of BES. Mixed-integer linear programming (MILP) is used in [50–51] to achieve these objectives. In [52], the optimal capacity of BES in a grid-connected PV system is accomplished by minimizing the cyclelife cost using mixed-

integer nonlinear programming (MINLP) whereas an improved PSO is used for unit commitment problems in [53] keeping in view various uncertainties and BES degradation. Following the above-mentioned literature, a BES aging model for local energy communities equipped with rooftop solar PV is addressed in [54]. Here, the knowledge of day-ahead load demand and PV power generation is considered to study the degradation performance of BES. Moreover, in [55] the day-ahead solar PV generation is forecasted using an autoregressive model followed by the BES degradation analysis of the Li-phosphate battery. However, none of the literature listed above analyses the degradation of residential BES with prior knowledge of forecasting and DRP participation together.

End-user consumers are motivated to participate in the electricity markets via DRP as it forms a link between retail and wholesale electricity markets [56]. It encourages consumers to reduce energy consumption against dynamic pricing announced day-ahead in a deregulated environment. End-users participate in the DRP by reducing the consumption during critical peaks without shifting loads with temporary discomfort in return for the incentives paid by the service provider (SP), known as EDRP or they can shift the load demand to other periods without any loss. Some relevant literature is documented here. The profit maximization of a compressed air energy storage, incorporating the market price uncertainty, is proposed in [57] for optimal bidding and offering strategies. An incentive-based DRP is modeled in [58] for a capacity market program such that load profile attributes like energy reduction, peak reduction, and peak to valley distance along with consumer benefits are considered. In [59], a similar work highlighting the consumer's participation is presented whereas reconfigurations in distributed networks are integrated with incentive-based DRP in [60]. Both the above-mentioned works incorporated microgrid uncertainties. To infuse realistic scenarios, the incentive-based and price-based DRP is demonstrated for real power markets [61] whereas the participation of EVs in the electricity market is documented in [62] for optimal parking management in a hydrogen-based intelligent parking lot using MINLP. A similar study is conducted in [63] for intelligent charging planning of EVs in commercial parking lots. Here, the nonlinear optimization is solved using CONOPT. Moreover, a comprehensive review of the optimal location of the EV charging station is reported in [64]. An optimal energy management strategy is developed using MILP in [65] with both EV and BES participating in the retail electricity market considering the uncertainties of EV, solar insolation, pool market, wind speed, and load demand. In [66–69], a scheduling strategy for a multi-energy microgrid in a wholesale electricity market is investigated as a bi-level optimization problem taking into account various storage devices, DRP, and uncertainties. Moreover, the impact of various DRPs on the residential energy community such as sizing of residential microgrids, home energy management systems, and optimal pricing is reported in [70–73]. The majority of literature documented above pertains to the wholesale electricity market while the industrial and commercial consumers are the major focus. In addition, the above-mentioned DRP mostly deals with the issues such as energy management, transmission

Table 2

A summary showing the comparison between existing literature and this study.

Reference	Uncertainty	Forecasting	DR	Degradation Analysis	Market Type	Storage Type	Solver
[47] [48] [49]	X	X	X	✓	—	Hybrid EV	PMP
[50]	X	X	X	✓	Retail	Residential BES	MILP
[51]	X	X	X	✓	Wholesale	Commercial BES	MILP
[52]	X	X	X	✓	Wholesale	Commercial BES	MINLP
[53]	✓	X	X	✓	Wholesale	Commercial BES	Improved PSO
[55]	X	✓	X	✓	Wholesale	Commercial BES	—
[57]	✓	X	X	X	Wholesale	Compressed Air	MILP
[62]	✓	X	✓	X	Wholesale	Hydrogen/EV	MINLP
[65]	✓	✓	✓	✓	Retail	EV/Commercial	MILP
[66]	✓	X	✓	X	Wholesale	Multiple	MILP
Proposed study	X	✓	✓	✓	Retail	Residential BES	GABC

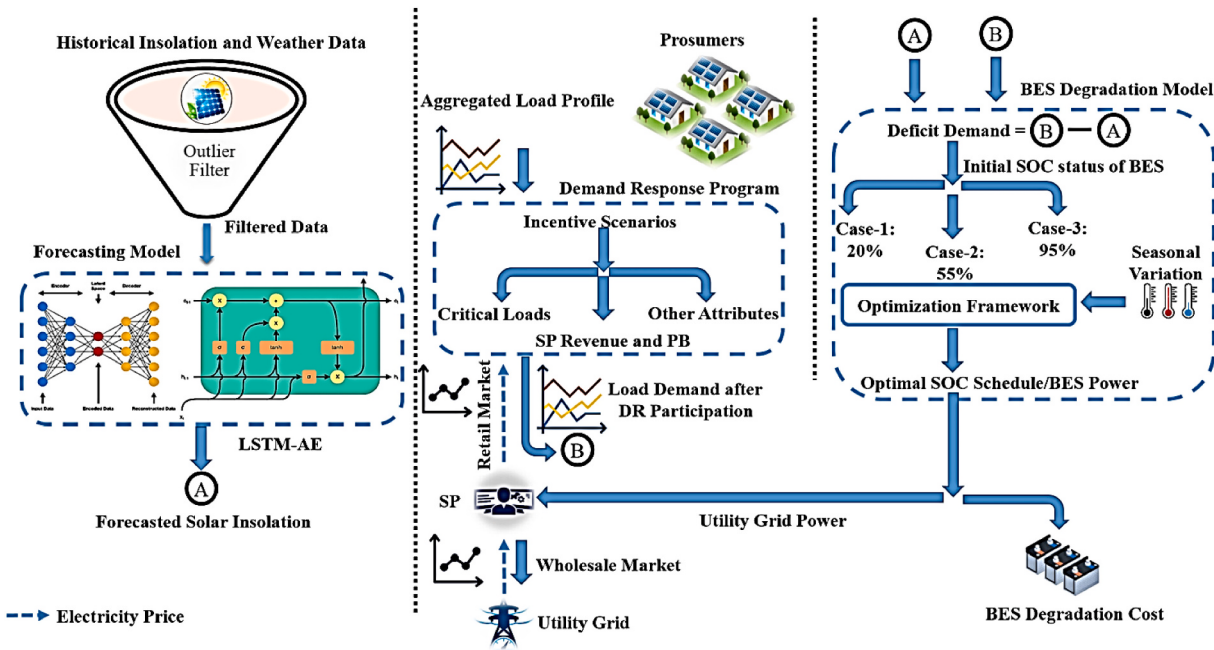


Fig. 1. Overall workflow of the proposed approach.

network planning, and security enhancement. However, the impact of DRP focusing on the local energy community issues such as BES degradation is open to research and is covered in this study.

1.2. Motivation

The research gap mentioned in the previous sub-section drives the authors to perform the present work. The scope of the presented study is explained here. This study combines forecasting, DRP, and BES degradation analysis under one roof. The proposed work demonstrates the insolation forecasting for residential prosumers based on outlier filtered LSTM-AE followed by the optimal degradation cost of BES subject to seasonal variations. The aforementioned objectives are achieved in the presence of an incentive-based EDRP with 100% prosumer participation. The selection of an incentive value is explored to achieve a revenue-benefit balance keeping critical loads intact.

The economic analysis in this work utilizes the prior information on solar PV generation and load demand at the residential/domestic level. The ambient temperature is the driving force and helps in an efficient BES aging model while the influence of C_{rate} and SOC is studied via severity factor mean. Furthermore, to explore the tuning of GABC, we are able to find parameters resulting in optimal solutions averaged over several trials while other meta-heuristic methods are compared on a common base. To the best of the author's knowledge, no such multi-dimensional work combining three different research areas have been presented to date. Since the power system is transiting towards a deregulated environment, intelligent BES wear models are desired for residential prosumers. Table 2 lists the outline of this study and its comparison with the existing literature. Based on this, the research gap identified concerning the optimal degradation cost of the BES may be summarized as follows:

- Proper microgrid planning in terms of forecasting energy vectors for BES degradation has not been studied, hence prior knowledge of the forecasted variable required to study the residential BES can be very crucial in the precise calculation of optimal degradation cost.
- Most of the literature documented above focuses on the cyclic aging model for hybrid EVs or various storage technologies and is limited to the service provider/utility grid end. However, these existing

works lack the active participation of residential prosumers, and their potential via the DRP remains undiscovered in the retail electricity market.

1.3. Contribution of this work

The research gap, mentioned above, forces us to propose an optimized BES aging model at the residential level with continuous support for critical demand for a resilient local energy community in the presence of an EDRP. This paper not only covers forecasting methodology but also allows prosumers to participate in EDRP. Moreover, the previous work [8], showcased the impact of cloud cover on load and solar insolation forecasting obtained with LSTM neural networks. To further investigate the significance of outliers and noise, an outlier filter alongside LSTM-AE neural network is incorporated for enhanced forecasting accuracy. The key contributions of this study are:

- Day-ahead solar insolation forecasting is performed for residential prosumers using one-class support vector machine (OCSVM) outlier filter-based LSTM-AE.
- Modeling of EDRP for residential prosumers and selection of suitable incentives based on the balance between SP revenue and prosumer benefit keeping critical loads intact is presented.
- A novel constraint is established to showcase the charging and discharging behavior of BES under various realistic conditions. The prerequisite knowledge of the available and deficit capacity during discharging mode and the remaining and surplus capacity during charging mode is utilized to limit the BES power within the boundary. Also, a penalty factor for the constraints violation is incorporated in this study.
- The optimal degradation cost of BES for residential prosumers with an assurance of uninterrupted aid to critical loads with and without EDRP using the GABC algorithm with optimal parameter settings is evaluated.

1.4. Organization of paper

The paper is arranged as follows. Section II introduces system modeling, forecasting methodology, modeling of EDRP, and modeling of

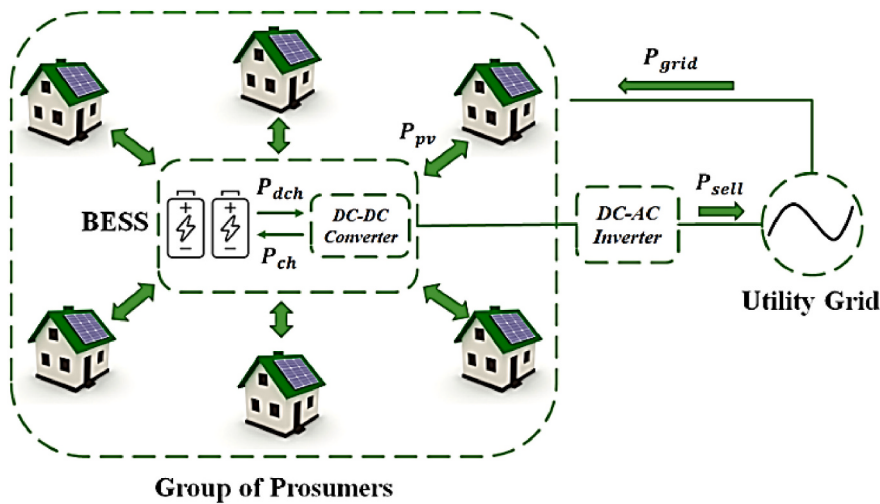


Fig. 2. System schematic for local energy community with grid-tied PV-BESS.

Table 3

System specifications for local energy community with grid-tied PV-BESS.

Component	Rating	Component	Rating
Connected Load	10 kW	Number of BES	12
Critical Load	20% of Connected Load	Total Capacity	25.92 kWh
PV Array	13 kW Peak	SOC Range	0.2–0.95
BES Voltage	12 V	Min. BES Power	Critical Load
BES Ah	180 Ah	Max. BES Power	Deficit Load

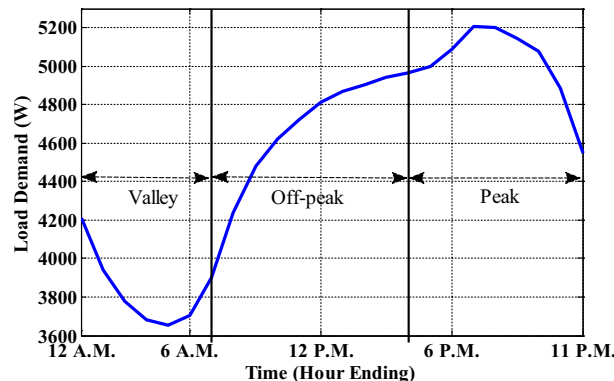


Fig. 3. Prosumer's aggregated load demand for any one day averaged over five years.

BES; Section III presents the proposed methodology and problem formulation; the GABC algorithm is comprehensively discussed in section IV; Section V involves discussion of the OCSVM-LSTM-AE forecasting, selection of incentive scenario, case studies carried out, and detailed discussion of results and Section VI concludes this work with limitations and future scope.

2. System modeling

2.1. Residential community system

The flow of the proposed work is depicted in Fig. 1. for the community microgrid model shown in Fig. 2. An OCSVM-LSTM-AE forecasting model is adopted for predicting the day-ahead solar insolation followed by modeling of DRP ensuring active participation of prosumers in the electricity market while the BES degradation cost is evaluated using a suitable optimization method and finally the performance of BES

Table 4

Parameters of the OCSVM-LSTM-AE forecasting model.

LSTM-AE model variables	
Inputs	Output
Hour of the day, seasonality, ambient temperature, relative humidity, wind speed, cloud amount, solar insolation, clearness index	Day-ahead insolation
OCSVM hyper-parameters	
Kernel	'rbf' (Default)
ν	0.01
γ	'auto'

is compared subject to various case studies. The group of prosumers is equipped with rooftop solar PV panels along with a BES system. In these prosumers, the DC-DC converter between PV and BES ensures the two-way flow of power (i.e. PV to BES and BES to loads) and also aids in charging (P_{ch}) and discharging (P_{dch}) of the BES. The overall PV-BES combination is tied to the utility grid via a bidirectional converter. System specifications are depicted in Table 3. Fig. 3 depicts the aggregated load demand profile of prosumers averaged over five years. The energy consumption data corresponds to the PJM region [74]. The 24 h. are split into valley period (12 A.M.–7 A.M.), off-peak period (7 A.M.–4 P.M.), and peak period (4 P.M.–11 P.M.).

BES, Battery energy storage; DR, Demand response; LSTM-AE, Long short-term memory autoencoder; PB, Prosumer benefit; SP, Service provider; SOC, State-of charge;

When an ample amount of solar insolation is available, the energy demand is fulfilled by solar PV (P_{pv}). The excess generation made by PV arrays aids in charging the BES (P_{ch}) while surplus power can be fed back to the grid (P_{sell}). Similarly, low solar insolation induced by poor climatic conditions causes deficit demand to be shared by BES (P_{dch}) and utility grid (P_{grid}) while an appropriate control algorithm makes sure that the critical loads are retained successfully.

2.2. Outlier filtered forecasting methodology

As the modern-day microgrid is equipped with DERs such as solar, wind, biomass, and BES along with several communication devices, a large portion of data is getting stored with the advancement in the data storage options. These datasets may encounter some bad or corrupted data points, also known as outliers, which may disturb the structure of the original time series resulting in degraded performance of the system.

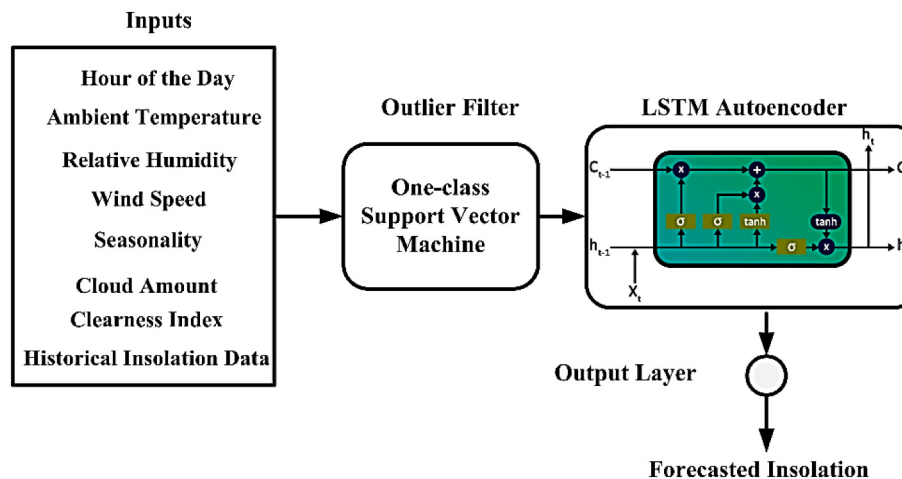


Fig. 4. OCSVM filter based LSTM-AE forecasting model architecture for this study.

To address this issue, an OCSVM-LSTM-AE-based day-ahead solar insolation forecasting for residential prosumers is presented. Autoencoder (AE) is good in dealing with both compact illustration and denoising of input while an OCSVM is used to filter the corrupted measurements. The tuning of AE is crucial for the optimal performance of the model. In this study, the selection of hidden layer neurons is achieved with the Keras tuner. It is implemented in the *Python-Jupyter notebook*. Energy consumption [74], solar insolation [75], and weather [76] datasets with the hourly resolution are available online. Table 4 lists the forecasting model details.

The overall architecture of the proposed model is depicted in Fig. 4. The input features with the hourly resolution are passed through the OCSVM filter as a part of the data cleaning process. The cleaned data is allowed to enter the encoder layer (LSTM), followed by a code layer and a decoder layer (LSTM). The structure of the encoder and decoder layers is the same while the code layer requires hyper-parameter tuning. The output layer gives the day-ahead forecasted solar insolation. The performance of this forecasting model is assessed using MAE, MBE, and R. Here, for simplicity, the concept of cloud cover is ignored and only sunny days are considered while forecasting.

In this work, residential consumers are considered as the energy-consuming entity in a local community. These consumers are furnished with rooftop solar PV arrays along with BES. The amount of critical loads in a residential building or a group of prosumers is limited such as lifts, water pumps, parking area, auxiliary supply to the BES control room, surveillance cameras, and other shared common spaces inside the premises. Thus, the selection of the BES rating is such that it guarantees uninterrupted assistance to these critical demands. The daily average energy consumed by critical load is found to be 19.001 kWh. Hence, a BES capacity of 25.920 kWh is selected with a series/parallel combination of 12 V, 180 Ah batteries. It ensures 24 h of energy backup if and only if critical load demand needs to be satisfied.

Furthermore, the charging and discharging behavior of the BES is influenced by load demand, ambient temperature, SOC, and C_{rate} . The influence of these aforementioned parameters on the BES aging model is discussed in the upcoming section followed by the objective function formulation for minimizing the degradation cost of the BES.

2.3. Emergency demand response program modeling

In a deregulated microgrid environment, DRP has opened many opportunities for cost-effective operation and efforts are being made to encourage consumer participation in the retail electricity market thus reducing supply-demand mismatch by adjusting non-critical loads on the demand side. Price elasticity of demand indicates how sensitive demand is to price as given by Eq. (1),

Table 5
EDRP parameters used in this study.

Parameters	Elasticity (peak)	θ	λ	d_{min}
Value	-0.1	3	5	Critical loads

$$E(m, n) = \frac{P_{ini}(n)}{d_{ini}(m)} \frac{\partial d(m)}{\partial P(n)} \quad (1)$$

To tackle the real-time price variations, the load demand is either shifted to other intervals or curtailed. In single-period modeling, loads are connected or disconnected but cannot be shifted to other intervals, hence known as self-elastic, whereas, in multi-period modeling, the loads are moved to the off-peak period thus reducing discomfort, hence known as cross-elastic. Accordingly, the prosumer's new load demand with EDRP in self-elasticity mode is modeled as,

$$d(m) = d_{ini}(m) \left\{ 1 + \frac{E(m, m)[P(m) - P_{ini}(m) + I(m) + Pen(m)]}{P_{ini}(m)} \right\} \quad (2)$$

where d_{ini} and d are the initial and new values of demand (kW) respectively, E is the elasticity, P_{ini} and P is the day-ahead and real-time price (€/kWh) respectively, I is the incentive price paid to the prosumers for demand reduction (€/kWh), Pen is the penalty (€/kWh) for disobeying the rules, and m, n are the periods.

In this study, an incentive-based EDRP involving 100% prosumers is implemented for peak reduction with a focus on single-period modeling. The incentives are varied in a wide range keeping penalty zero and an optimal value is chosen based on two factors; first, the load criticality, i.e. a capping of 20% is provided for critical loads such that the prosumers are entitled to consume at least these loads for higher values of incentives. Second, an appropriate balance between prosumer benefit and SP revenue is achieved. In addition, the reduction in energy consumption in response to incentives brings discomfort to the prosumers and the discomfort increases exponentially with the energy reduction (E_{red}). Here, the discomfort cost function (φ) [77] is given as,

$$\varphi = \frac{\theta}{2} \{E_{red}\}^2 + \lambda E_{red} \quad (3)$$

Here, θ and λ are the prosumer-dependent parameters and indicate their attitude towards EDRP [78] as listed in Table 5.

The prosumer's load demand after DR participation and forecasted PV generation is the key design variable in this study. These variables are input to the BES degradation model for computing the optimal SOC scheduling.

2.4. Mathematical modeling of battery energy storage

This sub-section presents the mathematical modeling of BES for the system being considered. A lithium-ion rechargeable BES converts the stored chemical energy into electrical energy during discharging mode and vice-versa during the charging mode of operation. The corresponding charging and discharging cell voltages are given as in (4) and (5),

$$V_{ch} = E_0 + V_{op+} + V_{op-} + IR_{pol} \quad (4)$$

$$V_{dis} = E_0 - V_{op+} - V_{op-} - IR_{pol} \quad (5)$$

Voltage-current model is considered the most vital sub-model for studying the BES, and it is the relation between terminal voltage and current [79]. Eq. (6) is shown below for constant-current discharge.

$$V_b = E_0 - K \left[\frac{Ah_{rated}}{Ah_{rated} - it} \right] i - R_0 i \quad (6)$$

where, E_0 is the open-circuit voltage (V), V_{op+} and V_{op-} are the over-voltage at the positive and negative electrodes respectively, R_{pol} is the polarization resistance, K is the polarization coefficient, Ah_{rated} is the rated ampere-hour capacity of BES, i is the battery current, and R_0 is the internal resistance of BES.

3. Proposed methodology

In this work, a single-objective optimization is proposed to minimize the degradation cost of BES in the presence of EDRP. The prosumer's day-ahead energy generation via solar PV is forecasted using OCSVM-LSTM-AE neural networks. The prosumer's day-ahead energy demand is average over five years for any one day. The energy demand after engaging in EDRP alongside PV generation is used to calculate deficit energy. Three case studies with different initial SOC of BES are conducted. The ambient temperature of three different seasons namely; summer, mild, and winter is considered to study its impact on cost. Finally, a tuned metaheuristic algorithm is used to solve the optimization problem. In the previous work reported in [49], the authors contributed to the overall cost optimization of plug-in hybrid electric buses. Here, the degradation performance of EV BES was studied with a major focus on the importance of cycle as well as calendar life. This section deals with the basics of the capacity fade phenomenon in BES highlighting the cycle-life model and various factors influencing its degradation via severity factor mean followed by the formulation of the objective function and constraints for BES degradation cost minimization.

3.1. Capacity fade model development

Lithium-ion exhibits exceptional thermal and chemical stability at a low cost, making it the best candidate for large-scale power applications. Due to the lack of operational data, the capacity fade behavior of such batteries has not been established but the primary reason behind capacity fade in a lithium-ion BES is the loss of active lithium caused by the degradation of the anode. To characterize the cyclife performance, numerous laboratory-based tests must be conducted to mimic the realistic conditions. Authors in [46] develop a cycle-life model to study the impact of temperature, depth of discharge, and C_{rate} but the dependency of SOC is neglected as may be observed in (7),

$$Q_{loss} = A \exp \left(\frac{-E_a}{RT} t^z \right) \quad (7)$$

where, A is the pre-exponential factor, E_a is the activation energy in J/mol , R is the gas constant, T is the temperature in K, z is the power-law factor and t is the time.

Suri et al. [47] fine-tuned the degradation model with the inclusion

Table 6
Details of fitting parameters for li-ion BES.

Parameter	Value	Parameter	Value
α	2896.6, $soc \leq 0.45$	E_a	31,500 J/mol
	2694.5, $soc > 0.45$	R	8.314
β	7411.2, $soc \leq 0.45$	z	0.57
	6022.2, $soc > 0.45$		
η	152.2		

Table 7
One-day temperature variation considered in this study

Parameter	Summer	Mild	Winter
Minimum	37.48 °C	12.48 °C	-12.52 °C
Maximum	39.57 °C	14.57 °C	-10.43 °C
Average	38.49 °C	13.49 °C	-11.50 °C

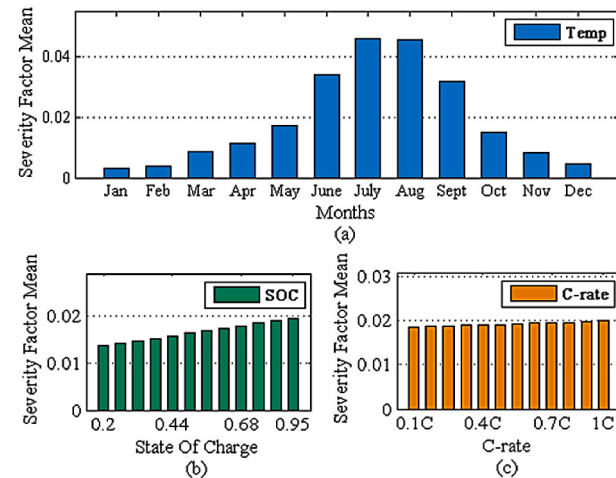


Fig. 5. Variation of Severity Factor Mean vs. (a) Monthly average temperature (b) SOC (c) C_{rate} .

of SOC for a hybrid EV Li-ion battery. The cycle-life model adopted in this paper is given as in (8),

$$Q_{loss} = (\alpha SOC + \beta) \exp \left(\frac{-E_a + \eta C_{rate}}{RT} \right) Ah^z \quad (8)$$

Here, the dependency on time ' t ' is replaced by ampere-hour throughput capacity, Ah . α and β are fitting coefficients and η is the compensation factor. The details of the fitting parameters [47] are listed in Table 6.

A graphical approach called *severity factor*, (σ) to showcase the impact of various parameters on the degradation of BES is developed in [47] to understand the relative aging of BES as given by (9),

$$\sigma(t) = \frac{Ah_{nom}(SOC_{nom}, C_{rate,nom}, T_{k,nom})}{Ah_{cyc}(SOC, C_{rate}, T)} \quad (9)$$

where Ah_{nom} indicates ampere-hour throughput under nominal conditions, i.e. $SOC_{nom} = 0.35$, $T_{k,nom} = 298.15$ K and $C_{rate,nom} = 1C$ and Ah_{cyc} indicates ampere-hour throughput when subjected to realistic conditions. Ah_{nom} and Ah_{cyc} can be represented as (10) and (11) respectively,

$$Ah_{nom} = \left\{ \frac{Q_{loss,EOL}}{(\alpha SOC_{nom} + \beta) \exp \left(\frac{-E_a + \eta C_{rate,nom}}{RT_{k,nom}} \right)} \right\}^{1/z} \quad (10)$$

$$Ah_{cyc} = \left\{ \frac{Q_{loss,EOL}}{(aSOC + \beta)exp\left(\frac{-E_a + \eta C_{rate}}{RT_k}\right)} \right\}^{1/z} \quad (11)$$

where, $Q_{loss,EOL}$ is considered to be 20% based on engineering experience and indicates the end of life (EOL) of BES. Eq. (10) can be used to calculate the nominal Ah-throughput for parameters depicted in Table 6 and it comes out to be 107,395 Ah. To achieve real conditions, the temperature corresponding to a single day located in the PJM region [75] in each of the summer, mild, and winter seasons is varied as shown in Table 7 and Eq. (11) is used to calculate Ah-throughput values. A higher value of severity factor is undesired and hints at faster degradation. Fig. 5 (a)-(c) shows the variation of severity factor mean versus monthly average temperature over the year, SOC, and C_{rate} respectively.

As it can be observed from Fig. 5, the mean value of the severity factor is relatively high during summer (July and August) when compared to mild (March–June and Sept.–Nov.) and winter (Dec., Jan., and Feb.) seasons while the impact of SOC (Fig. 5(b)) is moderate. But in Fig. 5(c), the severity factor mean is almost constant irrespective of the C_{rate} variation. As the BES degradation cost is least influenced by the C_{rate} , hence it is neglected in this study.

3.2. Problem formulation

The objective function is adopted from [48] and is expressed as follows:

$$f = \min(C_{bd}) \quad (12)$$

Where BES degradation cost (C_{bd}) is given by,

$$C_{bd} = \sum_{j=1}^{N_h} C_{bat} \frac{Ah_{eff}}{Ah_{nom}} \quad (13)$$

Eq. (9) can be re-written as,

$$Ah_{nom} = \sigma Ah_{cyc} \quad (14)$$

The EOL of a lithium-ion BES is reached such that the effective ampere-hour throughput is equal to the nominal ampere-hour throughput. Hence,

$$Ah_{eff} = \sigma Ah_{cyc} \quad (15)$$

If I_{bat} is the BES current during the charging/discharging hours N_h , then, the effective ampere-hour throughput, Ah_{eff} can be calculated as

$$Ah_{eff} = \sum_{j=1}^{N_h} \sigma(j)|I_{bat}(j)|\Delta t \quad (16)$$

Let C_{bat} be the cost of the BES inclusive of capital and installation cost. The BES degradation cost C_{bd} to be minimized for the j^{th} hour can be obtained using (13) as,

$$C_{bd} = \sum_{j=1}^{N_h} C_{bat} \frac{\sigma(j)|I_{bat}(j)|\Delta t}{Ah_{nom}} \quad (17)$$

In (17), I_{bat} takes into account both charging and discharging mode of operation and Δt is the time-step.

3.3. Operating constraints

3.3.1. Power flow constraints
In this work, prosumers with grid-tied rooftop PV-BES are considered. These rooftop PV panels will generate energy based on the available solar insolation to meet the residential energy demand while surplus PV power generation will be dispatched to BES and the utility grid [80]. Hence, the power flow equation is given by,

$$P_{load}(j) - P_{pv}(j) \mp P_{bat}(j) \mp P_{grid}(j) = 0 \quad (18)$$

where, P_{pv} and P_{load} are the forecasted PV generation obtained using OCSVM-LSTM-AE networks and actual demand respectively, P_{bat} with a positive value indicates the BES power during charging and that with a negative value indicates BES power during discharging mode and P_{grid} is the grid power where the positive sign convention hints at power fed back to the grid while the negative sign convention implies power demanded by the load.

3.3.2. BES power limit

A BES is integrated with the rooftop solar PV. Here, the rating of BES is selected such that it is capable of supplying at least critical load demand uninterruptedly for a duration of 24 h. under various disturbances, while shares deficit load demand under normal operating conditions. The limits are given as,

$$P_{bat}^{\min} \leq P_{bat}(j) \leq P_{bat}^{\max} \quad (19)$$

where, P_{bat}^{\min} is the minimum BES power and P_{bat}^{\max} is the maximum BES power as listed in Table 3.

3.3.3. BES state of charge

The BES SOC is considered to be the most vital parameter for analyzing its performance. From the knowledge of the initial status of the BES at any hour, the SOC at the next hour can be calculated as,

$$soc(j) = soc(j-1) \mp \frac{P_{bat}(j)\Delta j}{Q_{rated}} \quad (20)$$

where, Q_{rated} is the nominal rating of the BES as listed in Table 3.

In this work, it is assumed that the residential batteries can stockpile up to 95% and let go up to 20% of the nominal rating of the BES as shown in (21).

$$SOC_{\min} \leq soc(j) \leq SOC_{\max} \quad (21)$$

where, SOC_{\min} and SOC_{\max} are the lower and upper bounds of SOC.

3.3.4. Capacity constraint

A novel constraint is established to showcase the charging and discharging behavior of BES under various realistic conditions. The prerequisite knowledge of the available and deficit capacity during discharging mode and the remaining and surplus capacity during charging mode is utilized to limit the BES power within the boundary. This constraint is expressed as an available capacity constraint and remaining capacity constraint, given by (22) and (23) respectively. The minimum value of these two at any time instant will be used to calculate BES power under an optimized environment.

During charging mode:

$$Q_c = \min(Q_{rem}(j), Q_{surplus}(j)) \quad (22)$$

Or

During discharging mode:

$$Q_d = \min(Q_{avail}(j), Q_{def}(j)) \quad (23)$$

The BES power will be,

$$\sum_{j=1}^{N_h} P_{bat}(j) = Q_c \text{ or } Q_d \quad (24)$$

where, Q_{rem} and $Q_{surplus}$ are the remaining capacity of a BES and surplus capacity of the system at j^{th} hour during the charging mode of operation while Q_{avail} and Q_{def} are the available energy in a BES and deficit energy of the system at j^{th} hour during the discharging mode of operation.

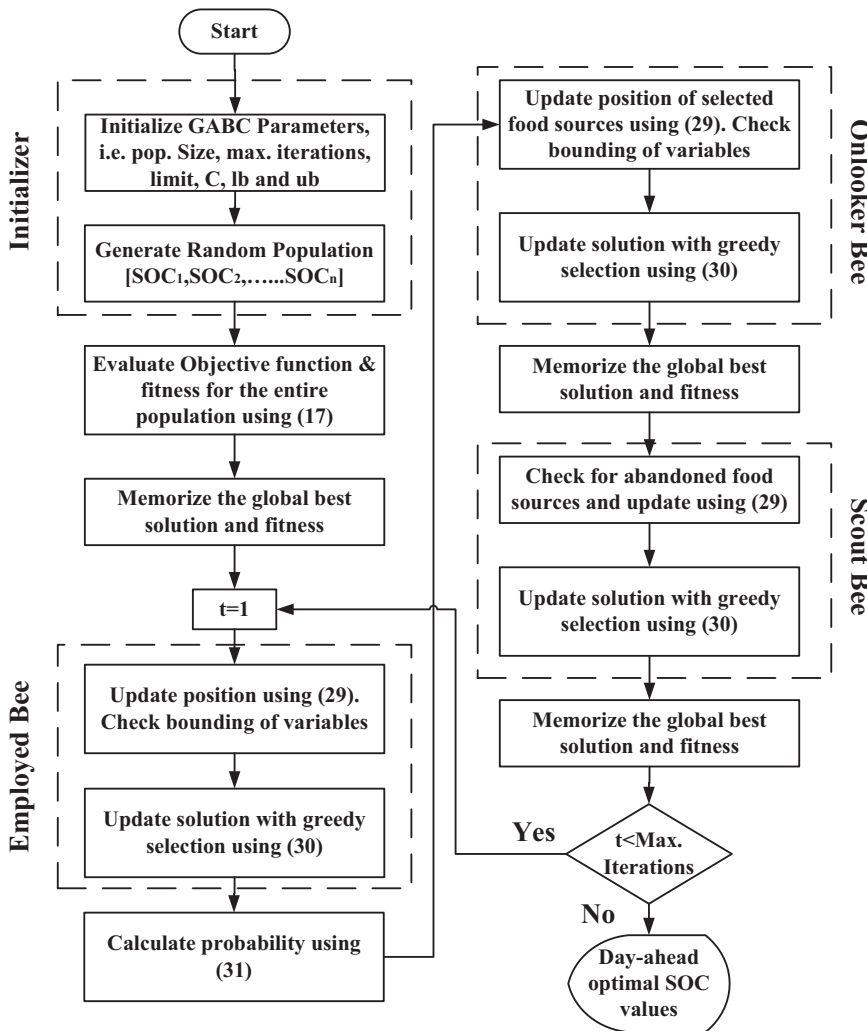


Fig. 6. Flowchart of GABC algorithm for day-ahead optimal SOC scheduling

3.4. Penalty factor

To incorporate the violation of constraints, a penalty factor is included as shown below,

$$\text{penalty} = \left| \frac{\sum P_{\text{bat}}}{Q_0} - 1 \right| \quad (25)$$

where, Q_0 is the capacity under either charging (Q_c) or discharging mode (Q_d).

From (17), it is clear that the BES degradation cost can be optimized under realistic conditions from the prior knowledge of actual load demand and forecasted PV power subject to the aforementioned constraints (18)–(24). These variables are used to calculate the deficit demand to be shared by BES and the utility grid. Here, SOC is considered to be the decision variable. Once the optimal value of SOC is obtained for the j^{th} hour, the corresponding BES power and C_{rate} can be calculated whereas the utility grid power is obtained as the difference between deficit demand and BES power. Also, based on these SOC scheduling, the Ah-throughput for the real environment is evaluated using (11) with fitting coefficients as per Table 6, followed by severity factor using (9) and the effective Ah-throughput using (16). It is to be noted here that a vector of 24 temperature values corresponding to 24 h. of the day is used for the calculation of Ah_{cyc} .

Finally, the degradation cost at each hour (either charging or discharging) is calculated using (13) till the termination criterion is

reached. Here, the ‘optimization framework’ is a generalized block indicating various techniques that can be adopted. The flowchart of the ‘optimization framework’ is depicted separately in the next section. In this work, the GABC algorithm is used to find out the degradation cost of BES and is compared with TLBO, Improved GWO [81], and PSO with inertia weight approach (PSO_IWA) [23] for showing the effectiveness of the proposed approach.

4. Gbest-guided artificial bee colony

ABC is a nature-inspired meta-heuristic optimization technique that utilizes the foraging behavior of honey bees in search of food sources. The entire process is split into three phases; employed bee, onlooker bee, and scout bee. Employed bees are the ones that currently exploit the food source and communicate with the other bees via waggle dance. The information shared by the employed bees is based on certain probabilities. Onlooker bees, on receiving information from employed bees, start searching for the selected food source. Both the above-mentioned phases adopt the greedy selection approach, i.e. if the new solution is better than the current solution, it memorizes the best solution while discarding the old one. A trail counter is used to record the number of failures, i.e. every time the new solution is not better than the current one, the trial counter is incremented by one while it is reset to zero for a better solution. Apart from this, a user-specified limit acts as a criterion for the scout bee phase. When the trial counter of at least one solution is greater than the limit, scout bees search for the food source. A detailed

flowchart of the GABC algorithm for optimal SOC scheduling is presented in Fig. 6.

In this work, GABC is implemented for obtaining minimized degradation cost of the BES in a grid-connected residential rooftop PV microgrid in a residential community in the presence of EDRP. The original characteristics of the ABC algorithm remain intact during the entire process as explained below.

Step 1: Firstly, the parameters such as objective function (f), population size (N_p), maximum iteration (T), limit, lower (lb), and upper bound (ub) of the decision variable are initialized.

Step 2: A random population X_{pop} is generated for problem dimension D by the GABC algorithm to initiate the process as given below,

$$X_{pop} = [x_1, x_2, \dots, x_k, \dots, x_{N_p}] \quad (26)$$

Step 3: Evaluate the fitness function 'fit', for the entire population as per (27),

$$fit = \begin{cases} \frac{1}{1 + |f|}, & f \geq 0 \\ 1 + |f|, & f < 0 \end{cases} \quad (27)$$

Each food source x_j for the i^{th} element is calculated between the lb and ub as,

$$x_k^i = lb^i + rand(0, 1)(ub^i - lb^i) \quad (28)$$

For $j \in 1 \dots N_p$; $i \in 1 \dots D$.

Step 4: Next, each bee in the employed bee phase exploits the food source and updates the new position x_{j+1}^i given by (29).

$$x_k^{i+1} = x_k^i + \phi(x_k^i - x_p^i) + \varphi(x_k^i - x_k^i) \quad (29)$$

where, x_k^i is the current solution, x_p^i is the partner solution for $p \neq j, i \in 1 \dots N_p$, x_i is the i^{th} element of the global best solution, \emptyset is a random number $[-1, 1]$ and φ is a random number $[0, C]$; C is a non-negative constant and plays a crucial role in balancing the exploration and exploitation feature of GABC.

Step 5: Step 3 is repeated to evaluate the fitness function.

Step 6: Greedy selection approach is used to update the solution as shown below,

If $fit_{new} > fit$,

$$\left. \begin{array}{l} X = x_k^{i+1} \\ f = f_{new} \end{array} \right\} \quad (30)$$

Step 7: The onlooker bees continue to search the selected food source based on the probability. Here, the probability is given by (31).

$$P_i = \frac{fit_i}{\sum_{k=1}^{N_p} fit_k} \quad (31)$$

where, fit_i is the fitness function for each solution.

Step 8: Step 4 to step 6 is repeated.

Step 9: Based on the trail counter in both the employed and onlooker bee phase, the scout bee phase is invoked if the $trial$ is greater than the $limit$. The best solution before the scout bee phase is memorized.

5. Results and discussion

In this work, the simulation study is carried out in PYTHON 3.7.4 and MATLAB R2010a software. The computations such as outlier filtering using OCSVM, fitting the LSTM-AE forecasting model, implementation of objective function and constraints, GABC algorithm and its tuning, and evaluation of all the results were obtained using a personal computer with an Intel Core i5 2nd generation processor having a 4 GB RAM and running on Windows 7 operating system. This section demonstrates the results obtained in a phase-wise manner i.e. forecasting of solar

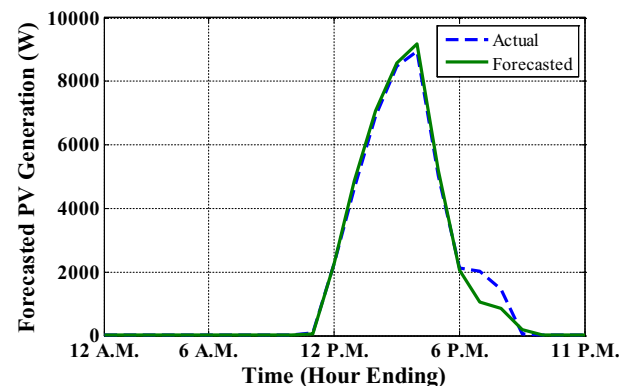


Fig. 7. PV power generation via forecasted insolation obtained using OCSVM-LSTM-AE

Table 8
Performance metrics of the OCSVM-LSTM-AE forecasting model

Model	MAE	MBE	R
OCSVM-LSTM-AE	0.0423	-0.0117	0.9840

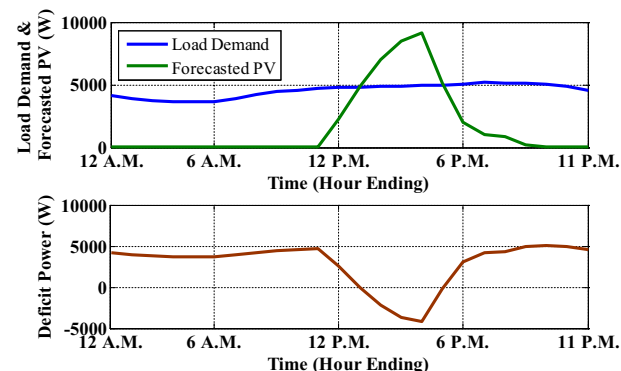


Fig. 8. Actual load demand, Forecasted PV power, and Deficit power

insolation for the residential community, participation of prosumers in the EDRP via incentive selection criterion, and performance analysis of BES degradation under the various initial status of BES and environmental conditions. Apart from this, the meta-heuristic techniques used in this work are tuned and compared for the optimal degradation cost of BES.

5.1. Solar insolation forecasting

Day-ahead forecasted PV power generation under various realistic conditions is obtained via OCSVM-LSTM-AE. Fig. 7 represents the PV generation forecasted using LSTM-AE with actual (in blue) and forecasted (in green) data. It can be observed that the outlier data points have a reasonable amount of impact on forecasting accuracy as the proposed model outclasses the model documented in the literature [8]. Table 8 lists the forecasting errors and model accuracy. The MAE and MBE of the forecasting model are found to be 0.0423 and -0.0117 respectively. The R-value is found to be 0.984, indicating a strong correlation between the actual and the forecasted variables.

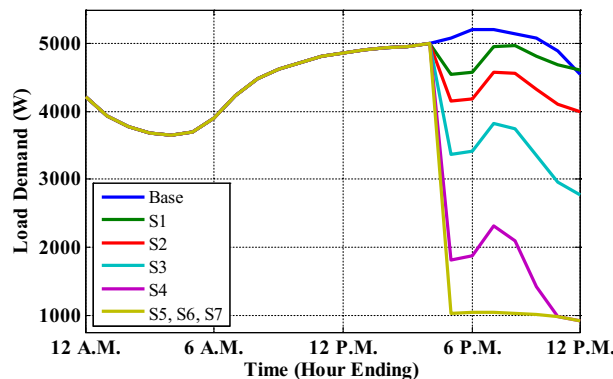
From the knowledge of load demand after DRP participation and day-ahead forecasted insolation, the amount of hourly deficit power can be calculated for a particular day as the difference between actual load and forecasted PV power generation as shown in Fig. 8. This deficit amount of power will be shared by the BES and the utility grid. The

Table 9

Incentive scenarios with load profile and economic attributes on prosumer participation in EDRP of Fig. 3

Incentive (cents/kWh)	Base	S ₁ 5	S ₂ 10	S ₃ 20	S ₄ 40	S ₅ 60	S ₆ 80	S ₇ 100
Load profile attributes								
Energy consumption (kWh)	109.587	107.586	104.349	97.869	85.821	81.456	81.456	81.456
Peak reduction (%)	–	12.104	19.497	34.295	63.892	80.00	80.00	80.00
Energy reduction (%)	–	1.825	4.779	10.692	21.686	25.669	25.669	25.669
Peak to valley distance (kW)	1.557	1.347	1.347	2.225	4.0881	4.0881	4.0881	4.0881
Load factor (%)	87.66	89.68	86.98	81.58	71.54	67.90	67.90	67.90
Economic attributes								
Prosumer bill (€)	555.79	543.21	525.52	489.91	422.46	394.28	394.28	394.28
Discomfort cost (€)	0	15.97	67.34	264.54	966.08	1327.7	1327.7	1327.7
DR cost (€)	0	12.12	56.05	239.33	987.63	2244.9	4011.1	6286.3
SP revenue (€)	555.79	531.16	469.47	250.57	-565.17	-1850.6	-3616.8	-5892.0
Prosumer benefit (€)	0	24.62	86.31	305.21	1120.96	2406.41	4172.6	6447.8

Note: Bold values indicate the selection of incentive scenario

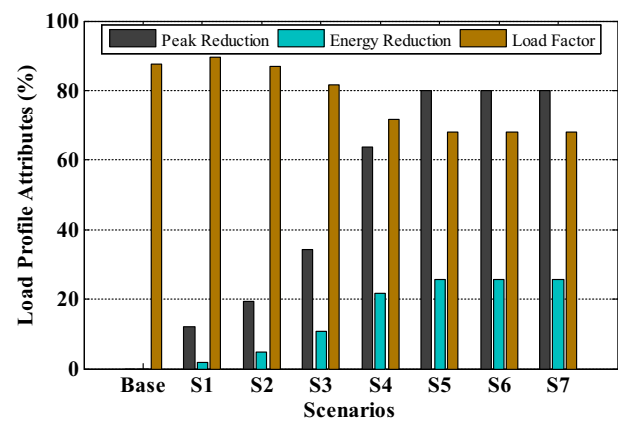
**Fig. 9.** Prosumers load demand after EDRP participation for various incentive scenarios

positive deficit power indicates the load demand to be satisfied by the BES and utility grid while negative power is the surplus PV generation used to charge the BES. Here, BES is designed keeping in mind the demand set by the critical loads. Depending on the initial status of BES, the discharging and charging hours will vary, for example, if the BES is fully charged at the inception of simulation, it discharges and shares power with the utility grid as per the load demand until the PV generation is sufficient enough to supply the load demand. Similarly, it starts charging when the PV generation is greater than the load demand.

5.2. Incentive selection via EDRP modeling.

To achieve a legitimate balance between PB and SP revenue, various incentive scenarios along with the base case are compared with each other based on the percentage of peak reduction, energy reduction, and load factor before choosing an optimal incentive value. Fig. 3 is used for EDRP modeling while the day-ahead and real-time electricity prices (for 24th October 2021) are accessed online. In this EDRP, the prosumers are committed to demand reduction such that only non-critical loads can be curtailed with minimum discomfort. The elasticity and customer-dependent parameters are listed in Table 5.

Apart from the BES degradation cost, the residential prosumers are entitled to pay for the electricity purchased from the utility grid. The amount of energy absorbed from the grid is calculated from Eq. (18) and the electricity price is announced by the system operator on a day-ahead basis in a deregulated market. The day-ahead and real-time electricity prices are available online and can be accessed via Commonwealth Edison Company [82]. Additionally, the prosumers' participation in EDRP brings cost on discomfort given by Eq. (3) while the cost of participating in EDRP is calculated as follows,

**Fig. 10.** Peak reduction, Energy reduction, and Load Factor vs. Incentive scenarios

$$C_{edrp} = I(m)(d_{ini}(m) - d(m)) \quad (32)$$

Assuming the penalty to be zero, using Eq. (2) in Eq. (32) yields the cost paid to the prosumer for EDRP participation,

$$C_{edrp} = -d_{ini}(m)E(m, m)I(m) \left[\frac{\{P(m) - P_{ini}(m)\} + I(m)}{P_{ini}(m)} \right] \quad (33)$$

Table 9 summarizes the economic aspects of the prosumer's energy consumption behavior in EDRP and the same has been compared with the base case scenario. The study was carried out with seven different incentive scenarios (S₁₋₇). The scenarios considered in this study along with various attributes of load profile are shown in **Table 9**. For instance, when the incentive is 20 €/kWh (S₃), the peak reduces by 34.295% while an energy reduction of 10.692% is observed. Moreover, the prosumer electricity bill slashes by 65.88 € while maintaining a balance between SP revenue and PB with a slight increase in discomfort. The load profile under EDRP is shown in Fig. 9 indicating active participation of prosumers in DRP while the attributes are illustrated in Fig. 10 and Fig. 11.

It can be observed that during the peak period as the prosumers participate in EDRP, the energy consumption reduces against the incentives provided by the SP keeping critical loads intact. Moreover, from S₄ onwards, the energy reduction, peak reduction, and load factor are almost constant irrespective of the incentives because of the load criticality capping provided by the SP.

Also, an increase in incentives beyond S₄ causes an exponential rise in the discomfort as can be seen in Fig. 11 (a) and from the viewpoint of economics, S₃ provides a good balance between the PB and SP revenue while higher incentives for SP will be in loss as visible from Fig. 11(b).

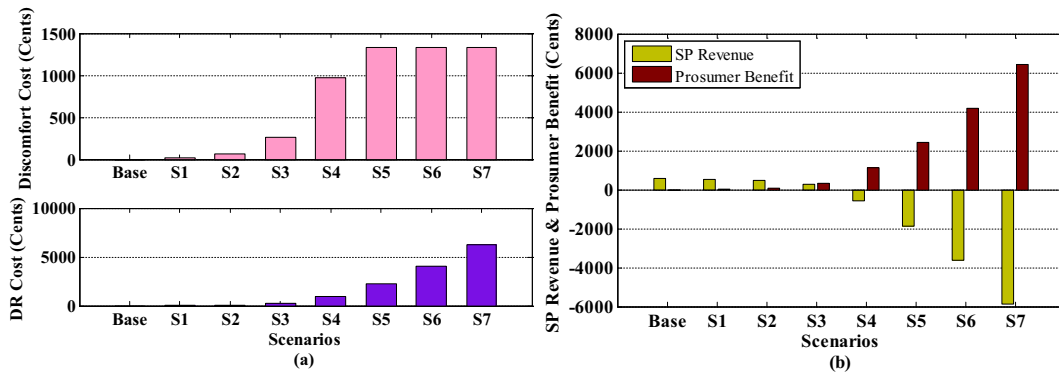


Fig. 11. (a)-(b) Discomfort cost, DR cost, SP revenue, and Prosumer Benefit vs. Incentive scenarios

Table 10
GABC tuning parameters considered in this study

Parameters	Values
Colony size	[10, 30, 50, 100, 200, 300, 400]
Employed/onlooker bees	Each 50% of colony size
Limit	[0, 0.0208 N_pD , 0.0416 N_pD , 0.0625 N_pD , 0.075 N_pD , 0.375 N_pD , N_pD]
Non-negative constant 'C'	[0.5, 1, 1.5, 2, 5]
Max. Iterations, T	100

Thus, in this study, S_3 is considered as the termination criterion and the BES degradation cost is evaluated for the same. SOC, C_{rate} , and temperature are the major parameters to assess the BES performance. Here, SOC is considered as the decision variable and the temperature variation is incorporated by considering three different days each from summer, winter, and mild conditions while the impact of C_{rate} on BES degradation performance is neglected as already discussed in section 3.1.

5.3. BES degradation cost with EDRP

5.3.1. GABC tuning parameters

GABC has few tuning parameters that adversely affect the system output and can be model-specific. Parameters such as colony size, number of employed and onlooker bees, limit, and non-negative constant C are tuned to yield the optimal solution. In this work, C, limit, and colony size are varied to incorporate their impact on BES degradation cost for each of the seasonal variations while the number of employed and onlooker bees are assumed to be the same and are equal to half of the colony size.

The role of the non-negative constant 'C' is to maintain the balance between the exploration and exploitation aspect of GABC, tuning of limit allows variation in the number of scout bees to exploit the abandoned food source, and variation in colony size helps the honey bees to forage in the different search space. Each of these tuning parameters is run for 10 trials and the moderate values yielding optimal solutions are considered. GABC tuning parameters [45,83] are listed in Table 10. Here, the non-negative constant 'C' is varied between 0.5 and 5, the limit varies as a percentage of the product of population size and the number of decision variables, and colony size has a range of 10 to 400.

Three case studies with initial SOC of 0.20, 0.55, and 0.95 are conducted. For each of the cases, the GABC parameters are optimally tuned,

Table 11
Impact of GABC tuning parameters on BES degradation cost with S_3

Tuning parameters	Degradation cost, €/day								
	(soc _{ini} = 0.20)			(soc _{ini} = 0.55)			(soc _{ini} = 0.95)		
	Summer	Mild	Winter	Summer	Mild	Winter	Summer	Mild	Winter
0.5	316.74	50.16	5.49	469.30	72.47	8.09	647.09	100.73	10.85
1	314.15	50.31	5.40	472.65	73.65	8.15	645.30	101.71	11.08
1.5	311.57	50.00	5.29	465.18	71.52	7.87	633.99	99.92	10.69
2	313.22	50.12	5.44	466.80	73.88	8.01	636.83	100.17	10.71
5	315.48	50.18	5.38	477.12	73.00	7.93	654.92	100.94	10.71
Limit									
0	344.99	51.69	5.73	474.54	73.51	8.10	656.95	103.69	11.22
0.0208 N_pD	335.19	50.56	5.35	474.73	71.75	7.82	650.23	100.62	10.72
0.0416N_pD	311.57	50.00	5.29	465.18	71.52	7.87	633.99	99.92	10.69
0.0625 N_pD	319.16	49.69	5.31	461.37	73.37	8.04	630.86	95.04	11.01
0.075 N_pD	302.38	47.76	5.31	474.50	72.80	8.05	628.42	98.10	10.53
0.375 N_pD	304.58	49.01	5.46	467.34	71.97	8.03	642.10	99.20	11.04
N_pD	314.12	49.46	5.44	480.24	74.02	7.85	645.62	99.67	10.82
Colony size									
10	252.04	39.84	4.63	474.37	64.43	7.09	559.98	92.07	9.98
30	296.12	44.87	5.02	440.92	68.10	7.64	611.24	98.10	10.27
50	287.95	44.73	5.32	464.98	72.89	7.47	644.06	98.14	10.45
100	311.57	50.00	5.29	465.18	71.52	7.87	633.99	99.92	10.69
200	325.66	53.59	5.86	494.77	74.37	7.95	666.58	102.78	11.14
300	321.77	52.30	5.75	473.05	77.64	8.33	663.20	99.98	11.12
400	336.92	48.98	5.73	471.37	76.14	8.07	659.72	104.91	11.14

Note: Bold values indicate the selection of GABC tuning Parameters through minimum degradation cost

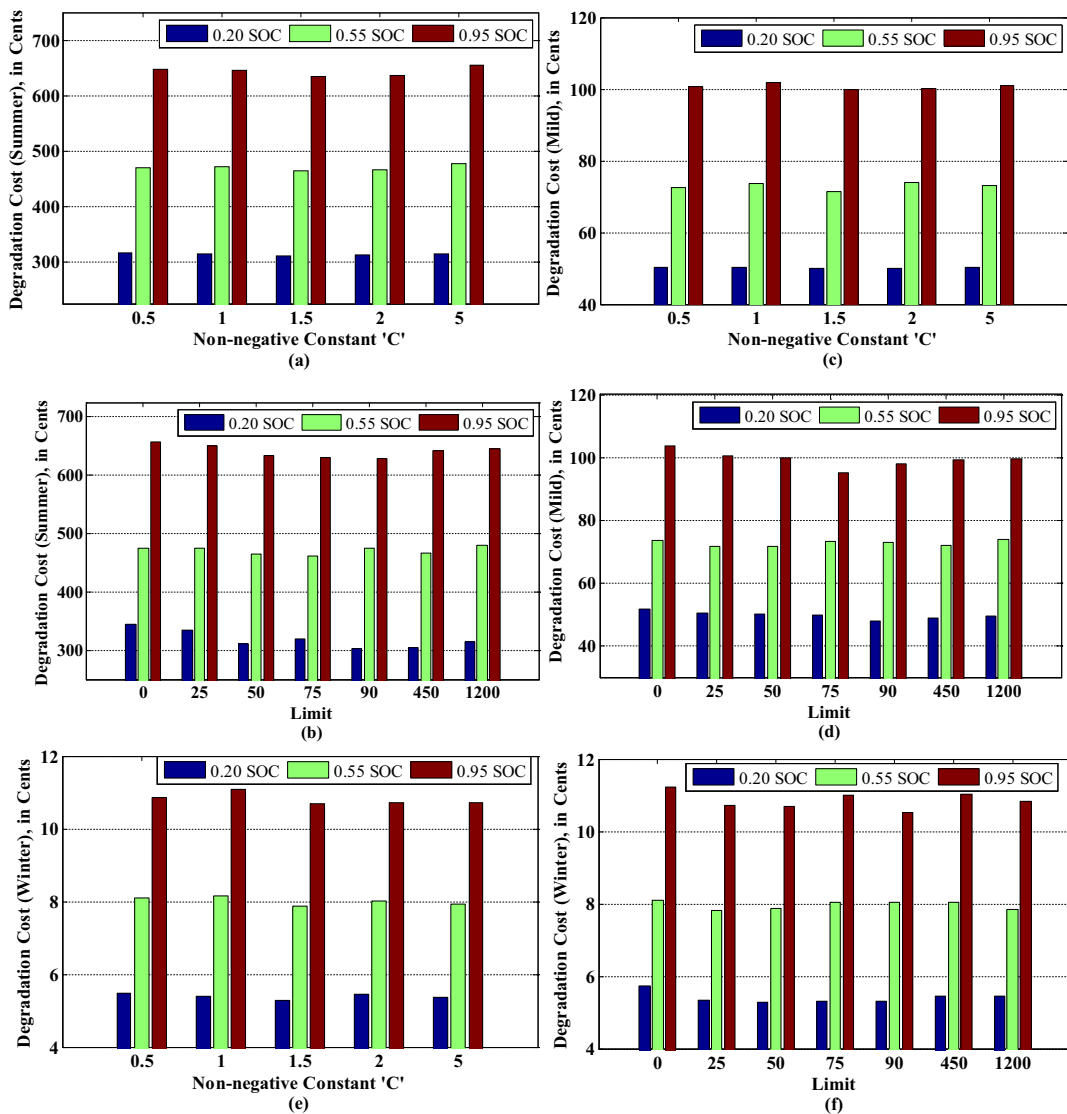


Fig. 12. Minimum average degradation cost obtained after GABC tuning for variation in 'C' and Limit (a)-(b) Summer (c)-(d) Mild, and (e)-(f) Winter for each of the case studies

and finally, the BES degradation cost is evaluated with and without EDRP for comparison and again is compared with the forecasted variables as obtained in [8]. Table 11 summarizes the BES degradation cost via tuning of GABC for S_3 obtained via EDRP. First, the non-negative constant is varied between 0.5 and 5, and the limit and colony size is held constant. For example, consider $soc_{ini} = 0.20$ on a summer day, the BES degradation cost at $C = 0.5$ is found to be 316.74 €/day which is less than 469.30 €/day, and 647.09 €/day at $soc_{ini} = 0.55$ and $soc_{ini} = 0.95$ respectively. It is because lower initial SOC of BES will encounter fewer discharging hours in a day when compared to the other two cases. Also, it is clear that, at $C = 1.5$, the algorithm yields the best solution (average value) as visible from Fig. 12 and the consistency of C can be seen with case-1 (Fig. 12(a)), case-2 (Fig. 12(c)), and case-3 (Fig. 12(e)) for all seasons.

Similarly, to incorporate the scout bee phase, the limit is varied from 0 to $N_p D$ while C and colony size are fixed. A lower value of limit indicates the algorithm failed to find the best solution whereas a higher value tends to explore more. For instance, considering a limit equal to 0, the GABC algorithm tries to exploit the solutions and ends up with the worst solutions in most of the cases as can be observed from Table 11, hence a moderate value of $0.0416N_p D$ is chosen as depicted in Fig. 12(b), Fig. 12(d), and Fig. 12(f) for summer, mild, and winter respectively.

Furthermore, the colony size is varied between 10 and 400 keeping other parameters fixed. It is observed that as the size of the colony increases, the BES degradation cost is also increased and remains almost constant for the higher number of bees with more computational time. Considering a colony size of 10, it can be demonstrated that although the computational time is the lowest to reach optimal solutions, the algorithm fails to explore while an increase in colony size to a moderate level considerably improves its ability to explore more i.e. a lower value of colony size reaches the optimal solution in quick time while the extra number of bees doesn't improve the solution, hence a moderate value of 100 is selected as shown in Fig. 13(a)-Fig. 13(c).

It is clear from the above observation that the tuning parameters play a vital role in analyzing the system performance, hence the optimal settings of these parameters are very important. Fig. 11- Fig. 13 demonstrate their impact on the model output and are consistent with the seasonal variation for each of the case studies. Based on the above study, $C = 1.5$, limit = 50, and colony size = 100 are chosen and the best solution is averaged over 10 trials.

5.3.2. Case-1: Initial SOC equal to SOC_{min}

In this case, it is assumed that the BES is fully discharged at the start of the simulation, i.e. $soc_{ini} = 0.20$. Fig. 14 displays the SOC of BES and

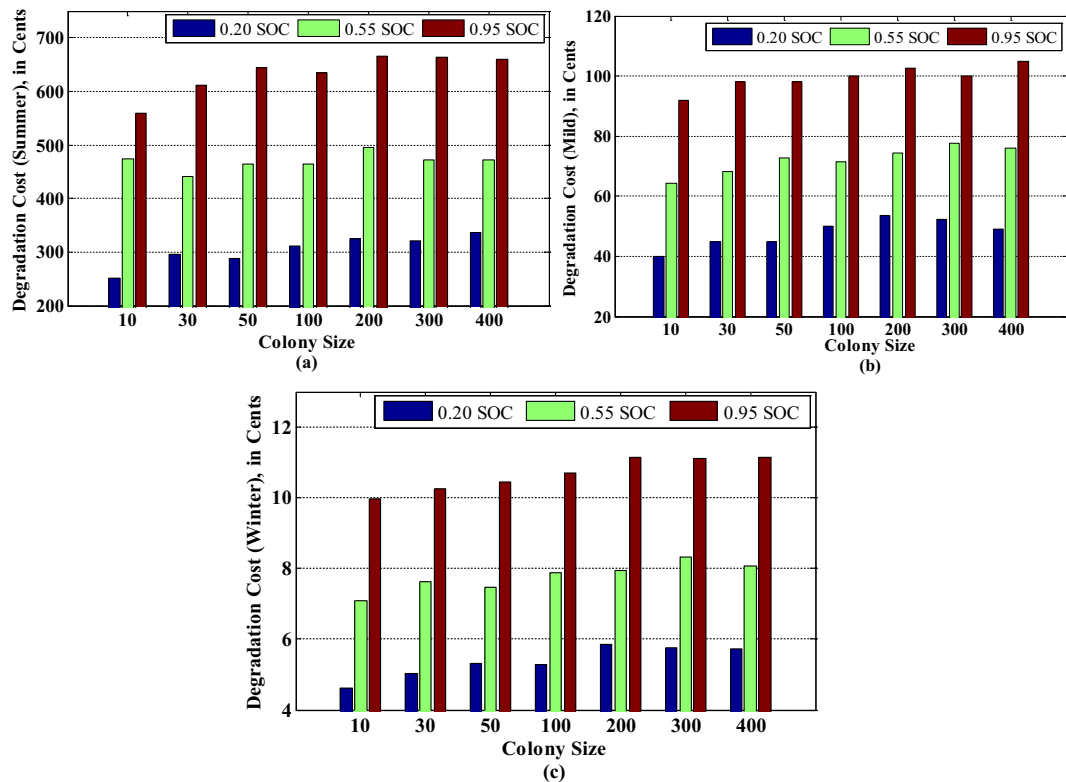


Fig. 13. Minimum average degradation cost obtained after GABC tuning for variation in Colony Size (a) Summer (b) Mild, and (c) Winter for each of the case studies

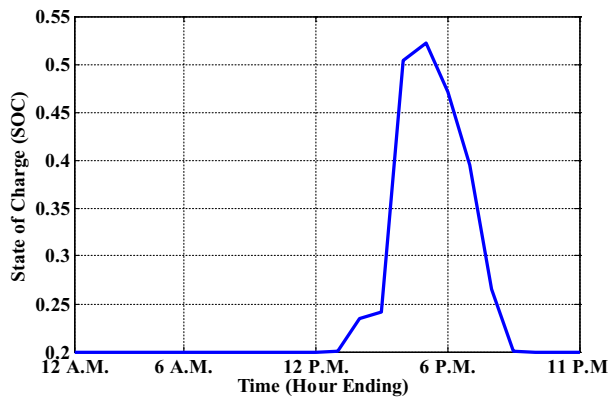


Fig. 14. One-day variation of SOC for case-1

Fig. 15 depicts the deficit power shared by the BES and the utility grid for this case. This causes the BES to stay in discharged mode (blue curve in **Fig. 15**) while load demand will be fulfilled by the utility grid (green curve in **Fig. 15**) until enough PV power generation is available to charge the BES to SOC_{max} or a value close to it based on the available solar insolation. Once BES is charged, it will share the prosumer's load demand alongside the utility grid for the rest of the day or until it gets discharged, whichever is earlier. Based on this assumption, the optimization framework generates day-ahead SOC values which are further used to calculate P_{bat} (Eq. (20)), Ah_{cyc} (Eq. (11)) and σ (Eq. (9)). Finally, the BES degradation cost corresponding to optimal SOC values is determined for S_3 of EDRP under a tuned environment as per **Table 11**. The daily best/worst/average cost obtained via GABC is 298.51 €/319.65€/311.57€ (summer), 43.23€/54.72€/50.00€ (mild), and 5.06€/5.60€/5.29€ (winter) respectively.

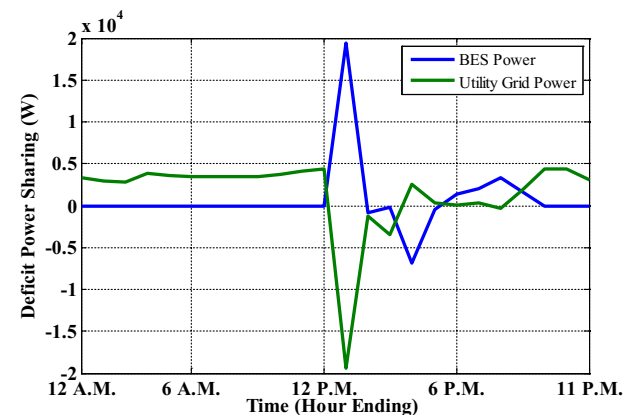


Fig. 15. Variation of BES power and utility grid power for case-1

5.3.3. Case-2: Initial SOC equal to $SOC_{min} \leq soc \leq SOC_{max}$

Unlike case-1, here it is assumed that the initial status of the BES is i.e. $soc_{ini} = 0.55$. **Fig. 16** shows the SOC plot and **Fig. 17** shows the deficit power shared by the BES and utility grid for the case considered. Given the situation, the BES will be discharged initially and reaches SOC_{min} (**Fig. 16**) depending upon the load demand and waiting for the PV power generation to get itself charged to SOC_{max} or lower value and continues to supply load demand for the rest of the day or until it reaches SOC_{min} . Using this assumption, the optimization framework is executed for determining the day-ahead SOC values. These SOC values are used to calculate the P_{bat} , Ah_{cyc} and σ as per Eq. (20), (11), and (9) respectively. As the BES degradation cost is a function of P_{bat} and Ah_{cyc} , the optimal degradation cost, in the presence of EDRP (S_3), is evaluated using an optimization algorithm. To study the impact of GABC tuning parameters on BES degradation cost for $soc_{ini} = 0.55$, a similar approach like case-1 is repeated here and an average value of BES degradation cost is chosen

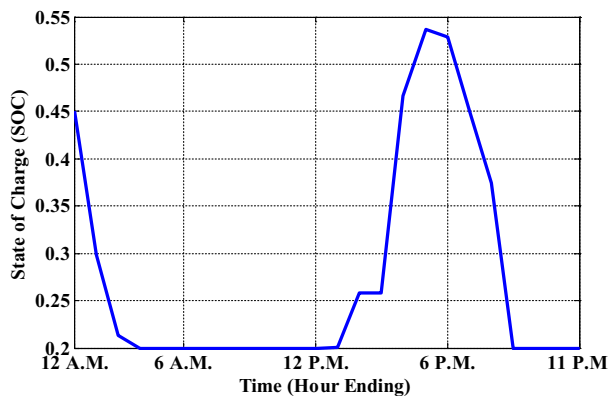


Fig. 16. One-day variation of SOC for case-2

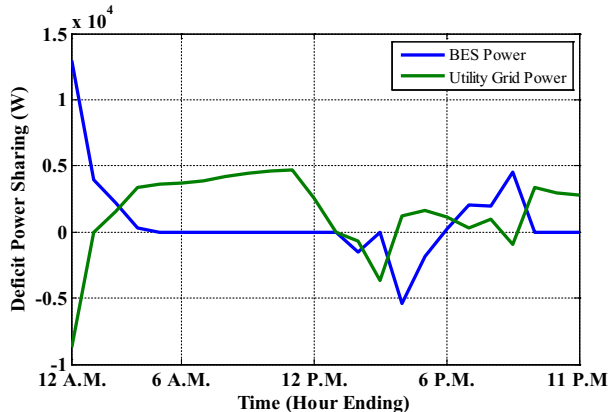


Fig. 17. Variation of BES power and utility grid power for case-2

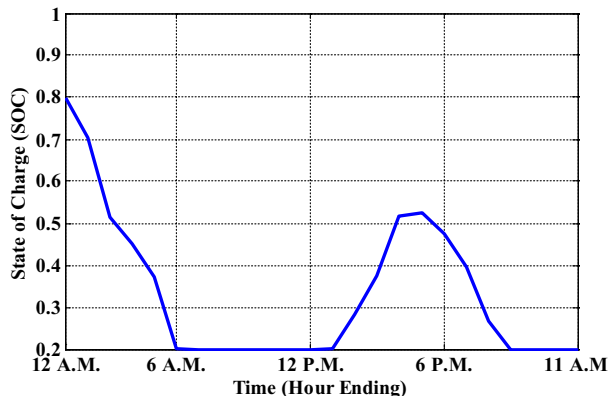


Fig. 18. One-day variation of SOC for case-3

with seasonal variations. The daily best/worst/average cost obtained via GABC is 449.09€/480.41€/465.18€ (summer), 69.04€/72.57€/71.52€ (mild), and 7.52€/8.22€/7.87€ (winter) respectively.

5.3.4. Case-3: Initial SOC equal to SOC_{max}

Furthermore, another assumption is that the BES is fully charged since the inception of simulation, i.e. $SOC_{max} = 0.95$. Fig. 18 illustrates the SOC variation and Fig. 19 illustrates the deficit power-sharing exhibited by BES and the utility grid. For this scenario, the BES (blue curve) continues to satisfy load demand alongside the utility grid (green curve) till it reaches SOC_{min} or a sufficient amount of PV power

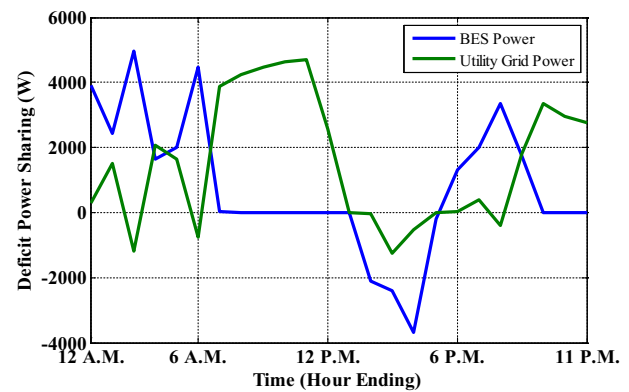


Fig. 19. Variation of BES power and utility grid power for case-3

generation is available to satisfy the load demand and charge the BES. During the absence of PV power generation, BES and the utility grid continues to share the load demand. All the steps of case-1 and case-2 are repeated here and the optimal degradation cost of BES, with prosumer-participated EDRP, is determined. Table 12 depicts the comparison of the proposed approach of outlier filter-based forecasting with the one reported in the literature. The daily best/worst/average cost obtained via GABC is 609.58€/649.07€/633.99€ (summer), 98.36€/100.94€/99.92€ (mild), and 10.10€/11.24€/10.69€ (winter) respectively. It can be observed that the degradation cost of BES subject to seasonal variations is further minimized with the inclusion of the OCSVM filter with EDRP.

5.4. Discussion of results

The comparative summary of BES degradation cost based on seasons, initial BES status, and metaheuristic methods is shown in Table 12. All the optimization methods are tuned and compared for the same number of iterations and colony size/population. The case studies discussed above demonstrate the advantages of proper microgrid planning at the community level, i.e. forecasting and the impact of prosumer participation in the retail electricity market via EDRP. For instance, for case-2, the optimal BES degradation cost via GABC with only prior knowledge of forecasted variable during summer is 642.41 €/day. This cost is further reduced to 529.4 €/day when the forecasting is performed in the presence of an outlier filter but without EDRP. Moreover, when the prosumers participate in the EDRP, the degradation cost further slashes to 465.18 €/day. This indicates that precise microgrid planning and encouraged prosumer participation has a reasonable economic impact, thus creating a balanced and fair environment between SP and prosumer. Moreover, the GABC algorithm with optimal tuning parameter settings outclasses TLBO, IGWO, and PSO_IWA delivering the best value of BES degradation cost with moderate computational time and is consistent for summer, mild, and winter seasons. It is to be noted here that each of the algorithms is implemented for the same number of colony sizes and iterations.

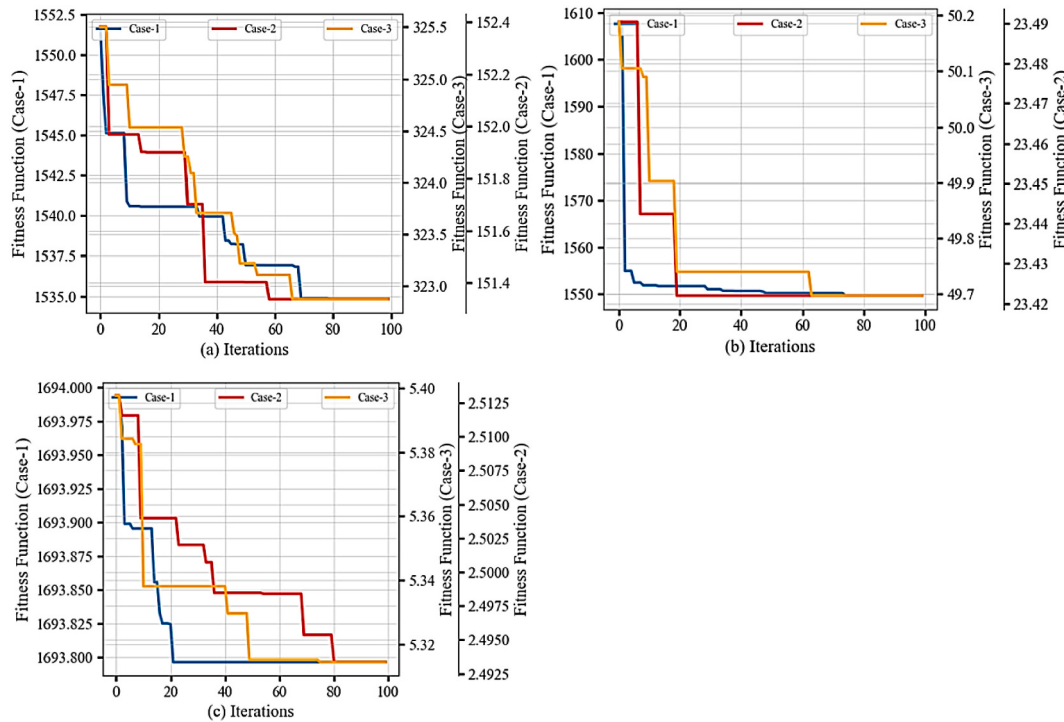
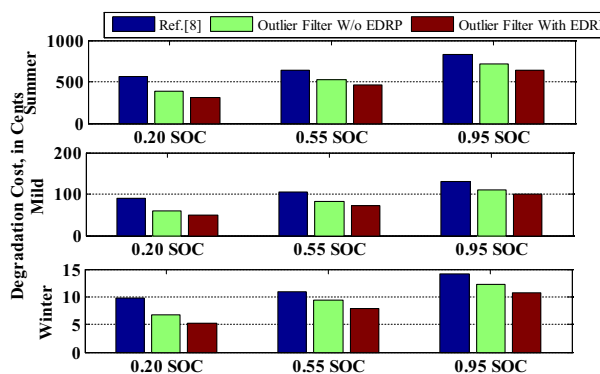
Fig. 20(a)-20(c) illustrates the fitness function variation of case-1 (in Blue), case-2 (in Red), and case-3 (in Orange) with iterations for summer, mild, and winter respectively. Here, three y-axes correspond to the fitness for each of the cases. Fig. 21 shows the bar plot for the overall cost comparison of the proposed study. The BES degradation cost with only the forecasting model in the absence of EDRP showcases the highest degradation cost (blue bar) for each of the case studies and is consistent with the seasonal variation whereas a slight improvement in cost (green bar) is observed when an outlier filter is incorporated to the existing forecasting model. Additionally, when prosumers engage in the market via EDRP, the degradation cost further sinks (brown bar) and shows the lowest degradation cost. The efficacy of the proposed methodology can be validated by the fact that the BES degradation cost is minimum for all

Table 12

Seasonal-wise comparison of BES degradation cost with and without EDRP for each of the case studies and various metaheuristic methods

Degradation cost, €/day											
Cases	Methods	Ref. [8] (C = 1, limit = 50, colony size = 100)			Outlier filter without EDRP (C = 1, limit = 50, colony size = 100)			Outlier filter with EDRP (C = 1.5, limit = 50, colony size = 100)			Time (s)
		Summer	Mild	Winter	Summer	Mild	Winter	Summer	Mild	Winter	
Case-1 0.20soc	TLBO	699.28	109.72	12.09	476.4	74.65	8.21	387.106	60.56	6.64	72
	IGWO	646.20	101.44	11.22	450.4	69.93	7.70	374.08	58.56	6.45	42
	PSO_IWA	585.42	92.98	9.82	404.9	64.01	6.93	341.28	54.30	5.92	31
Case-2 0.55soc	GABC	561.56	90.83	9.79	383.3	59.63	6.68	311.57	50.00	5.29	36
	TLBO	770.47	120.29	13.17	627.6	97.89	10.7	539.54	83.98	9.16	72
	IGWO	712.54	113.62	12.14	604.3	93.64	10.2	525.93	82.12	8.93	42
Case-3 0.95soc	PSO_IWA	661.62	109.04	12.11	534.0	86.0	9.51	500.70	78.35	8.18	31
	GABC	642.41	104.72	10.84	529.4	82.94	9.33	465.18	71.52	7.87	36
	TLBO	942.78	146.82	16.02	800.0	124.4	13.5	714.80	110.9	12.07	72
Case-3 0.95soc	IGWO	895.23	139.34	15.27	755.9	120.8	13.0	702.51	109.1	11.84	42
	PSO_IWA	870.55	133.89	15.01	715.3	110.3	12.5	664.59	102.8	11.32	31
	GABC	823.24	129.43	14.06	713.8	109.6	12.1	633.99	99.92	10.69	36

Note: Bold values indicate the superiority of GABC

**Fig. 20.** Fitness function Vs. Iterations (a) Summer (b) Mild (c) Winter**Fig. 21.** Cost comparison with and without EDRP for summer, mild, and winter for each of the case studies

the cases and seasons as summarized in **Table 13**. As high as 20% savings in daily BES degradation cost is evident for the proposed methodology when compared without EDRP. In addition to this, it is also visible that the amount saved is inversely proportional to both initial SOC and seasonal variation in most of the cases, i.e. least during summer and increases with a decrease in temperature. Similarly, lower initial SOC has lesser charging/discharging hours, hence lower cost and more savings. These savings can partially compensate for the loss of comfort experienced by the prosumers for EDRP participation.

It can be inferred that the participation of prosumers in the EDRP not only helps in energy reduction against the incentives with a small loss in comfort but also scales down the deficit energy to be borne by the BES. This in turn reduces the charging/discharging behavior, resulting in lesser degradation and extended cycle-life of the battery. Besides, operating BES at a higher temperature for a long time will have a negative economic impact i.e. more degradation costs in summer. This leads to a reduced cyclelife of the BES but the overall ampere-hour

Table 13

Overall comparison of BES degradation cost and percentage savings with and without EDRP using GABC for each of the case studies

Degradation cost, €/day												
Ref. [8]			Outlier filter without EDRP			Outlier filter with EDRP			Savings (%)			
	0.20soc (Case-1)	0.55soc (Case-2)	0.95soc (Case-3)	0.20soc (Case-1)	0.55soc (Case-2)	0.95soc (Case-3)	0.20soc (Case-1)	0.55soc (Case-2)	0.95soc (Case-3)	0.20soc (Case-1)	0.55soc (Case-2)	0.95soc (Case-3)
Summer	561.56	642.41	823.24	383.36	529.45	713.86	311.57	465.18	633.99	18.72	12.14	11.18
Mild	90.83	104.72	129.43	59.63	82.94	109.66	50.00	71.52	99.92	16.15	13.77	8.88
Winter	9.79	10.84	14.06	6.68	9.33	12.17	5.29	7.87	10.69	20	15.65	12.16

Note: Bold values indicate the superiority of the proposed approach and daily savings

handling capacity will improve over time. Likewise, at relatively mild or lower temperatures BES will be subjected to less stress, hence degradation costs will be low as compared to summer.

Furthermore, the proposed scheme has the potential for a real local energy community. The modern-day grid encourages consumers to opt for rooftop solar PV-BES systems to maximize their self-consumption. The future grid requires intelligent forecasting techniques for residential consumers. Proper planning of on-site generation ensures effortless local energy management between PV, energy storage, and the utility grid. Moreover, the surplus PV generation can be used as a peer to peer trading for the welfare of the entire community. Additionally, the consumers can actively engage in the retail market via DR participation and can avail social and economic benefits with minimum discomfort. Apart from static energy storage, the scheme can be a feasible choice for EV batteries such that grid-to-vehicle and vehicle-to-grid analysis can be performed with the proposed methodology.

6. Conclusion

In this paper, a novel framework for optimizing the degradation cost of the lithium-ion BES for a residential community furnished with rooftop solar PV has been proposed. A single-objective optimization has been presented for minimizing the total degradation cost of BES subject to variations in initial SOC and temperature. Here, LSTM-AE neural network with an OCSVM filter has been used for the prediction of day-ahead solar energy generation for a group of residential prosumers. The MAE, MBE, and R of the forecasting model have been found to be 0.0423, -0.0117, and 0.984 respectively. Besides, the impact of EDRP on BES degradation has been studied by assuming 100% prosumer participation, and various scenarios have been created for the selection of an incentive, based on several load profiles and economic attributes. An incentive of 20 €/kWh has been chosen to balance the SP revenue and PB. The forecasted solar PV generation and load demand after EDRP participation have been used as inputs to the proposed BES degradation model. The deficit energy demand has been taken care of by BES and the utility grid while continuous assistance to critical load has been assured in the study. The impact of SOC, temperature, and C_{rate} on the degradation of BES has been incorporated while modeling BES aging. Moreover, a unique constraint has been proposed considering the available and remaining capacity of a BES for charging/discharging mode. Finally, the GABC algorithm generates a day-ahead optimal SOC schedule which has been used to evaluate the BES degradation cost. Three case studies with initial SOC of 20%, 55%, and 95% with seasonal variations have been conducted in this study. The amount of savings experienced by the prosumers with precise forecasting methodology and engagement with the retail electricity market have been 18.78%, 12.14%, and 11.18% for summer, 16.15%, 13.77%, and 8.88% for mild, and 20%, 15.65%, and 12.16% for winter respectively. Furthermore, the following points indicate the observations and findings obtained during this study:

- The residential rooftop solar insolation forecasted using outlier filtered LSTM-AE improves the forecasting accuracy.

- The inclusion of incentive-based EDRP for peak and energy reduction influences the charging/discharging of BES resulting in lower degradation costs.
- 20 €/kWh has been selected as the trade-off between PB and SP revenue. Higher incentive values cause more discomfort, hence load criticality capping is important.
- In this study, to replicate the real-world scenario, the daily temperature corresponding to each of the seasons, i.e. summer, mild, and winter have been chosen and its impact on the BES degradation has been studied. Cooler/milder ambiance is found to be more economical than a warm day.
- The impact of GABC tuning parameters on BES degradation cost has been successfully investigated. An optimal setting of these parameters have been found to be $C = 1.5$, limit = 50, and colony size = 100 which yield minimum average degradation cost i.e. 311.57€ (summer), 50.00€ (mild), and 5.29€ (winter) for case-1, 465.18€ (summer), 71.52€ (mild), and 7.87€ (winter) for case-2, and 633.99€ (summer), 99.92€ (mild), and 10.69€ (winter) for case-3. The proposed framework with GABC has been proficient and produces an optimal solution with moderate computational time. To validate this, it has been compared alongside TLBO, IGWO, and PSO_IWA where the effectiveness of GABC over others is visible.
- Prosumer participation in EDRP cuts down as high as 20% of BES degradation cost as compared without EDRP.
- Initial SOC of BES and temperature have been the driving forces for BES degradation.

Temperature: lower temperature yield maximum savings.

Lower initial SOC: BES will get charged only in the presence of PV. Being in idle condition for prolong time causes negligible degradation, hence maximum savings.

The novelties and findings of the proposed work can be used as a research direction in the area of planning, demand-side management, and energy storage technologies. Load forecasting has not been considered in this work whereas the EDRP is applied for the aggregated load demand of prosumers, which will be extended and implemented for individual prosumers with a fair EDRP policy and an unbiased incentive distribution in the future to upgrade the proposed scheme. Apart from this, the design and formulation of a controller for the successful implementation of the proposed scheme can be realised. In this work, the case study has been conducted with ambient temperatures approximately ranging from -11 °C to +40 °C and is not location-specific. This brings a limitation to this study as the extreme temperatures may jump beyond these limits and are subject to geographical locations. Apart from this, the study can be extended further with any initial SOC value within the lower and upper bounds and the performance of the BES aging model can be evaluated. Besides, the study can be extended with a different type of BES for hybrid EVs, variable customer participation, and can be implemented for a price-based DR program.

Funding details

This research did not receive any specific grant from funding agencies in the public, commercial, or not-for-profit sectors.

Data availability

Datasets related to this article can be found at <https://www.kaggle.com/>, hosted at Kaggle [74–76], and <https://hourlypricing.comed.com/live-prices/>, hosted at Commonwealth Edison Company [82].

CRediT authorship contribution statement

Dipanshu Naware: Methodology, Writing – original draft, Visualization. **Raviteja Badigenchala:** Conceptualization, Software. **Arghya Mitra:** Writing – review & editing, Validation. **Debapriya Das:** Supervision.

Declaration of competing interest

The authors declare that they have no known competing financial interests or personal relationships that could have appeared to influence the work reported in this paper.

References

- [1] IEA, Global Energy Review 2021, IEA, Paris. <https://www.iea.org/reports/global-energy-review-2021>, 2021. (Accessed 12 November 2021).
- [2] IEA, Renewable electricity generation increase by technology, country and region, 2020–2021, IEA, Paris. <https://www.iea.org/data-and-statistics/charts/renewable-electricity-generation-increase-by-technology-country-and-region-2020-2021>. (Accessed 12 November 2021).
- [3] M. Alhussein, K. Aurangzeb, S.I. Haider, Hybrid CNN-LSTM model for short-term individual household load forecasting, *IEEE Access* 8 (2020) 180544–180557, <https://doi.org/10.1109/ACCESS.2020.3028281>.
- [4] K. Amarasinghe, D.L. Marino, M. Manic, Deep neural networks for energy load forecasting, in: *IEEE Int. Symp. Ind. Electron.*, IEEE, 2017, pp. 1483–1488, <https://doi.org/10.1109/ISIE.2017.8001465>.
- [5] V. Suresh, P. Janik, J.M. Guerrero, Z. Leonowicz, T. Sikorski, Microgrid energy management system with embedded deep learning forecaster and combined optimizer, *IEEE Access* 8 (2020) 202225–202239, <https://doi.org/10.1109/ACCESS.2020.3036131>.
- [6] M. Mir, M. Shafeezadeh, M.A. Heidari, N. Ghadimi, Application of hybrid forecast engine based intelligent algorithm and feature selection for wind signal prediction, *Evol. Syst.* 11 (4) (2020) 559–573, <https://doi.org/10.1007/s12530-019-09271-y>.
- [7] F. Mirzapour, M. Lakzaei, G. Varamini, M. Teimourian, N. Ghadimi, A new prediction model of battery and wind-solar output in hybrid power system, *J. Ambient. Intell. Humaniz. Comput.* 10 (1) (2019) 77–87, <https://doi.org/10.1007/s12652-017-0600-7>.
- [8] D. Naware, A. Mitra, Weather classification-based load and solar insolation forecasting for residential applications with LSTM neural networks, *Electr. Eng.* (2021), <https://doi.org/10.1007/s00202-021-01395-2>.
- [9] S.K. Aditya, D. Das, Application of battery energy storage system to load frequency control of an isolated power system, *Int. J. Energy Res.* 23 (3) (1999) 247–258, [https://doi.org/10.1002/\(SICI\)1099-114X\(19990310\)23:3<247::AID-ER480>3.0.CO;2-T](https://doi.org/10.1002/(SICI)1099-114X(19990310)23:3<247::AID-ER480>3.0.CO;2-T).
- [10] S.K. Aditya, D. Das, Battery energy storage for load frequency control of an interconnected power system, *Electr. Power Syst. Res.* 58 (3) (2001) 179–185, [https://doi.org/10.1016/S0378-7796\(01\)00129-8](https://doi.org/10.1016/S0378-7796(01)00129-8).
- [11] M.B. Roberts, A. Bruce, I. MacGill, Impact of shared battery energy storage systems on photovoltaic self-consumption and electricity bills in apartment buildings, *Appl. Energy* 1 (245) (2019 Jul) 78–95, <https://doi.org/10.1016/j.apenergy.2019.04.001>.
- [12] M.R. Jannesar, A. Sedighi, M. Savaghebi, J.M. Guerrero, Optimal placement, sizing, and daily charge/discharge of battery energy storage in low voltage distribution network with high photovoltaic penetration, *Appl. Energy* 15 (226) (2018 Sep) 957–966, <https://doi.org/10.1016/j.apenergy.2018.06.036>.
- [13] J. Koskela, A. Rautiainen, P. Järventauska, Using electrical energy storage in residential buildings—Sizing of battery and photovoltaic panels based on electricity cost optimization, *Appl. Energy* 1 (239) (2019 Apr) 1175–1189, <https://doi.org/10.1016/j.apenergy.2019.02.021>.
- [14] D. Ouyang, J. Weng, M. Chen, J. Wang, Impact of high-temperature environment on the optimal cycle rate of lithium-ion battery, *J. Energy Storage* 28 (2020), 101242, <https://doi.org/10.1016/j.est.2020.101242>.
- [15] S. Barcellona, L. Piegar, Effect of current on cycle aging of lithium ion batteries, *J. Energy Storage* 29 (2020), 101310, <https://doi.org/10.1016/j.est.2020.101310>.
- [16] M. Woody, M. Arbabzadeh, G.M. Lewis, G.A. Keoleian, A. Stefanopoulou, Strategies to limit degradation and maximize Li-ion battery service lifetime—critical review and guidance for stakeholders, *J. Energy Storage* 28 (2020), 101231, <https://doi.org/10.1016/j.est.2020.101231>.
- [17] S. Vonsien, R. Madleiner, Li-ion battery storage in private households with PV systems: analyzing the economic impacts of battery aging and pooling, *J. Energy Storage* 29 (2020), 101407, <https://doi.org/10.1016/j.est.2020.101407>.
- [18] K. Tantrapon, P. Jirapong, P. Thararak, Mitigating microgrid voltage fluctuation using battery energy storage system with improved particle swarm optimization, *Energy Rep.* 1 (6) (2020 Feb) 724–730, <https://doi.org/10.1016/j.egyr.2019.11.145>.
- [19] C. Jankowiak, A. Zacharopoulos, C. Brandoni, P. Keatley, P. MacArtain, N. Hewitt, Assessing the benefits of decentralised residential batteries for load peak shaving, *J. Energy Storage* 32 (2020), 101779, <https://doi.org/10.1016/j.est.2020.101779>.
- [20] A. Barré, B. Deguilhem, S. Grolleau, M. Gérard, F. Suard, D. Riu, A review on lithium-ion battery ageing mechanisms and estimations for automotive applications, *J. Power Sources* 1 (241) (2013 Nov) 680–689, <https://doi.org/10.1016/j.jpowsour.2013.05.040>.
- [21] M. Dubarry, N. Qin, P. Brooker, Calendar aging of commercial li-ion cells of different chemistries—a review, *Curr. Opin. Electrochem.* 1 (9) (2018) 106–113, <https://doi.org/10.1016/j.jcoelec.2018.05.023>.
- [22] M.M. Kabir, D.E. Demirocak, Degradation mechanisms in Li-ion batteries: a state-of-the-art review, *Int. J. Energy Res.* 41 (14) (2017) 1963–1986, <https://doi.org/10.1002/er.3762>.
- [23] R. Roy, S.P. Ghoshal, A novel crazy swarm optimized economic load dispatch for various types of cost functions, *Int. J. Electr. Power Energy Syst.* 30 (2008) 242–253, <https://doi.org/10.1016/j.ijepes.2007.07.007>.
- [24] A.S. Fraser, Simulation of genetic systems by automatic digital computers ii. Effects of linkage on rates of advance under selection, *Aust. J. Biol. Sci.* 10 (4) (1957) 492–500, <https://doi.org/10.1071/B19570492>.
- [25] M. Mehrpooya, N. Ghadimi, M. Marefat, S.A. Ghorbanian, Numerical investigation of a new combined energy system includes parabolic dish solar collector, Stirling engine and thermoelectric device, *Int. J. Energy Res.* 45 (11) (2021 Sep) 16436–16455, <https://doi.org/10.1002/er.6891>.
- [26] D. Karaboga, An idea based on honey bee swarm for numerical optimization, in: *Technical Report-tr06*, Erciyes University, Engineering Faculty, Computer Engineering Department, 2005.
- [27] S. Mirjalili, S.M. Mirjalili, A. Lewis, Grey wolf optimizer, *Adv. Eng. Softw.* 69 (2014) 46–61, <https://doi.org/10.1016/j.advengsoft.2013.12.007>.
- [28] R.V. Rao, V.J. Savsani, J. Balic, Teaching–learning-based optimization algorithm for unconstrained and constrained real-parameter optimization problems, *Eng. Optim.* 44 (2012) 1447–1462, <https://doi.org/10.1080/0305215X.2011.652103>.
- [29] X.S. Yang, *Nature-inspired Metaheuristic Algorithms*, Luniver press, 2010.
- [30] X.S. Yang, S. Deb, Engineering optimisation by cuckoo search, *Int. J. Math. Model. Numer. Optim.* 1 (4) (2010) 330–343.
- [31] S. Mirjalili, A. Lewis, The whale optimization algorithm, *Adv. Eng. Softw.* 1 (95) (2016) 51–67, <https://doi.org/10.1016/j.advengsoft.2016.01.008>.
- [32] A. Faramarzi, M. Heidarnejad, S. Mirjalili, A.H. Gandomi, Marine predators algorithm: a nature-inspired metaheuristic, *Expert Syst. Appl.* 152 (2020 Aug 15), 113377, <https://doi.org/10.1016/j.eswa.2020.113377>.
- [33] M.O. Badawy, F. Cingoz, Y. Sozer, BES storage sizing for a grid tied PV system based on operating cost minimization, in: *ECCE 2016 - IEEE Energy Convers. Congr. Expo. Proc.*, IEEE, 2016, pp. 1–7, <https://doi.org/10.1109/ECCE.2016.7854896>.
- [34] M. Fatnani, D. Naware, A. Mitra, in: *Design of Solar PV Based EV Charging Station With Optimized BES Energy Storage System*. 2020 IEEE First Int. Conf. Smart Technol. Power, Energy Control, Nagpur, Maharashtra, India, IEEE, 2020, pp. 1–5, <https://doi.org/10.1109/STPEC49749.2020.9297719>.
- [35] Z. Yang, M. Ghadamyari, H. Khoramdel, S.M. Alizadeh, S. Pirouzi, M. Milani, F. Banihashemi, N. Ghadimi, Robust multi-objective optimal design of islanded hybrid system with renewable and diesel sources/stationary and mobile energy storage systems, *Renew. Sustain. Energ. Rev.* 148 (2021), 111295, <https://doi.org/10.1016/j.rser.2021.111295>.
- [36] D. Sadeghi, N. Amiri, M. Marzband, A. Abusorrah, K. Sedraoui, Optimal sizing of hybrid renewable energy systems by considering power sharing and electric vehicles, *Int. J. Energy Res.* (2022 Feb 9), <https://doi.org/10.1002/er.7729>.
- [37] L.A. Wong, V.K. Ramachandaramurthy, S.L. Walker, P. Taylor, M.J. Sanjari, Optimal placement and sizing of battery energy storage system for losses reduction using whale optimization algorithm, *Journal of Energy Storage*. 26 (2019 Dec 1), 100892, <https://doi.org/10.1016/j.est.2019.100892>.
- [38] Y. Zhu, C. Liu, K. Sun, D. Shi, Z. Wang, Optimization of battery energy storage to improve power system oscillation damping, *IEEE Trans. Sustain. Energy* 10 (3) (2018) 1015–1024, <https://doi.org/10.1109/TSTE.2018.2858262>.
- [39] P. Singh, N.K. Meena, A. Slowik, S.K. Bishnoi, Modified African buffalo optimization for strategic integration of battery energy storage in distribution networks, *IEEE Access* 8 (2020) 14289–14301, <https://doi.org/10.1109/ACCESS.2020.2966571>.
- [40] H.U.R. Habib, U. Subramaniam, A. Waqar, B.S. Farhan, K.M. Kotb, S. Wang, Energy cost optimization of hybrid renewables based V2G microgrid considering multi objective function by using artificial bee colony optimization, *IEEE Access* 8 (2020) 62076–62093, <https://doi.org/10.1109/ACCESS.2020.2984537>.
- [41] M. Marzband, F. Azarinejad, M. Savaghebi, J.M. Guerrero, An optimal energy management system for islanded microgrids based on multiperiod artificial bee Colony combined with markov chain, *IEEE Syst. J.* 11 (2017) 1712–1722, <https://doi.org/10.1109/JSYST.2015.2422253>.
- [42] G. Zhu, S. Kwong, Gbest-guided artificial bee colony algorithm for numerical function optimization, *Appl. Math. Comput.* 217 (2010) 3166–3173, <https://doi.org/10.1016/j.amc.2010.08.049>.
- [43] M. Dixit, Impact of optimal integration of renewable energy sources and electric vehicles in practical distribution feeder with uncertain load demand, *Int. Trans. Electr. Energy Syst.* 30 (2020) 1–28, <https://doi.org/10.1002/2050-7038.12668>.
- [44] N.K. Paliwal, A.K. Singh, N.K. Singh, A day-ahead optimal energy scheduling in a remote microgrid alongwith BES storage system via global best guided ABC algorithm, *J. Energy Storage* 25 (2019), 100877, <https://doi.org/10.1016/j.est.2019.100877>.

- [45] C. Rathore, R. Roy, Impact of wind uncertainty, plug-in-electric vehicles and demand response program on transmission network expansion planning, Int. J. Electr. Power Energy Syst. 75 (2016) 59–73, <https://doi.org/10.1016/j.ijepes.2015.07.040>.
- [46] J. Wang, P. Liu, J. Hicks-Garner, E. Sherman, S. Soukiazian, M. Verbrugge, et al., Cycle-life model for graphite-LiFePO₄ cells, J. Power Sources 196 (2011) 3942–3948, <https://doi.org/10.1016/j.jpowsour.2010.11.134>.
- [47] G. Suri, S. Onori, A control-oriented cycle-life model for hybrid electric vehicle lithium-ion batteries, Energy 96 (2016) 644–653, <https://doi.org/10.1016/j.energy.2015.11.075>.
- [48] L. Tang, G. Rizzoni, S. Onori, Energy management strategy for HEVs including BES life optimization, IEEE Trans. Transp. Electrif. 1 (2015) 211–222, <https://doi.org/10.1109/TTE.2015.2471180>.
- [49] S. Zhang, X. Hu, S. Xie, Z. Song, L. Hu, C. Hou, Adaptively coordinated optimization of battery aging and energy management in plug-in hybrid electric buses, Appl. Energy 256 (2019), 113891, <https://doi.org/10.1016/j.apenergy.2019.113891>.
- [50] A. Yoshida, T. Sato, Y. Amano, K. Ito, Impact of electric battery degradation on cost-and-energy-saving characteristics of a residential photovoltaic system, Energy Build. 15 (124) (2016) 265–272, <https://doi.org/10.1016/j.enbuild.2015.08.036>.
- [51] M. Amini, A. Khorsandi, B. Vahidi, S.H. Hosseiniyan, A. Malakmohamadi, Optimal sizing of battery energy storage in a microgrid considering capacity degradation and replacement year, Electr. Power Syst. Res. 195 (2021), 107170, <https://doi.org/10.1016/j.epsr.2021.107170>.
- [52] Y. Wu, Z. Liu, J. Liu, H. Xiao, R. Liu, L. Zhang, Optimal battery capacity of grid-connected PV-battery systems considering battery degradation, Renew. Energy 1 (181) (2022) 10–23, <https://doi.org/10.1016/j.renene.2021.09.036>.
- [53] Jordehi A. Rezaee, An improved particle swarm optimisation for unit commitment in microgrids with battery energy storage systems considering battery degradation and uncertainties, Int. J. Energy Res. 45 (1) (2021) 727–744, <https://doi.org/10.1002/er.5867>.
- [54] R. Badigenchala, D. Naware, A. Mitra, in: Modelling of Lithium-ion BES Ageing for a Local Energy Community. 2021 Int. Conf. Intell. Technol., Hubli, IEEE, 2021, pp. 1–6, <https://doi.org/10.1109/CONITS1480.2021.9498346>.
- [55] M. Lee, J. Park, S.I. Na, H.S. Choi, B.S. Bu, J. Kim, An analysis of battery degradation in the integrated energy storage system with solar photovoltaic generation, Electronics 9 (4) (2020) 701, <https://doi.org/10.3390/electronics9040701>.
- [56] M.H. Albadri, E.F. El-Saadany, A summary of demand response in electricity markets, Electr. Power Syst. Res. 78 (11) (2008) 1989–1996, <https://doi.org/10.1016/j.epsr.2008.04.002>.
- [57] W. Cai, R. Mohammaditab, G. Fathi, K. Wakil, A.G. Ebadi, N. Ghadimi, Optimal bidding and offering strategies of compressed air energy storage: a hybrid robust-stochastic approach, Renew. Energy 1 (143) (2019) 1–8, <https://doi.org/10.1016/j.renene.2019.05.008>.
- [58] H.A. Aalami, M.P. Moghaddam, G.R. Yousefi, Demand response modeling considering interruptible/curtailable loads and capacity market programs, Appl. Energy 87 (1) (2010) 243–250, <https://doi.org/10.1016/j.apenergy.2009.05.041>.
- [59] M.H. Imani, P. Niknejad, M.R. Barzegaran, The impact of customers' participation level and various incentive values on implementing emergency demand response program in microgrid operation, Int. J. Electr. Power Energy Syst. 1 (96) (2018) 114–125, <https://doi.org/10.1016/j.ijepes.2017.09.038>.
- [60] P. Harsh, D. Das, Energy management in microgrid using incentive-based demand response and reconfigured network considering uncertainties in renewable energy sources, Sustain. Energy Technol. Assess. 46 (2021), 101225, <https://doi.org/10.1016/j.seta.2021.101225>.
- [61] M. Rahmani-andebili, Modeling nonlinear incentive-based and price-based demand response programs and implementing on real power markets, Electr. Power Syst. Res. 1 (132) (2016) 115–124, <https://doi.org/10.1016/j.epsr.2015.11.006>.
- [62] J. Liu, C. Chen, Z. Liu, K. Jermsittiparsert, N. Ghadimi, An IGDT-based risk-involved optimal bidding strategy for hydrogen storage-based intelligent parking lot of electric vehicles, J. Energy Storage 27 (2020), 101057, <https://doi.org/10.1016/j.est.2019.101057>.
- [63] M.A. Baherifard, R. Kazemzadeh, A.S. Yazdankhah, M. Marzband, Intelligent charging planning for electric vehicle commercial parking lots and its impact on distribution network's imbalance indices, Sustain. Energy Grids Netw. 24 (2022), 100620, <https://doi.org/10.1016/j.segan.2022.100620>.
- [64] F. Ahmad, A. Iqbal, I. Ashraf, M. Marzband, Optimal location of electric vehicle charging station and its impact on distribution network: a review, Energy Rep. 1 (8) (2022) 2314–2333, <https://doi.org/10.1016/j.egyr.2022.01.180>.
- [65] S. Zeynali, N. Rostami, A. Ahmadian, A. Elkamel, Stochastic energy management of an electricity retailer with a novel plug-in electric vehicle-based demand response program and energy storage system: a linearized battery degradation cost model, Sustain. Cities Soc. 74 (2021), 103154, <https://doi.org/10.1016/j.scs.2021.103154>.
- [66] N. Nasiri, S. Zeynali, S.N. Ravadanegh, M. Marzband, A hybrid robust-stochastic approach for strategic scheduling of a multi-energy system as a price-maker player in day-ahead wholesale market, Energy 235 (2021), 121398, <https://doi.org/10.1016/j.energy.2021.121398>.
- [67] S.M. Kazemi-Razi, H.A. Abyaneh, H. Nafisi, Z. Ali, M. Marzband, Enhancement of flexibility in multi-energy microgrids considering voltage and congestion improvement: robust thermal comfort against reserve calls, Sustain. Cities Soc. 74 (2021), 103160, <https://doi.org/10.1016/j.scs.2021.103160>.
- [68] N. Nasiri, S. Zeynali, S.N. Ravadanegh, M. Marzband, A tactical scheduling framework for wind farm-integrated multi-energy systems to take part in natural gas and wholesale electricity markets as a price setter, IET Gen. Transm. Distrib. 16 (9) (2022) 1849–1864, <https://doi.org/10.1049/gtd2.12423>.
- [69] S.E. Ahmadi, D. Sadeghi, M. Marzband, A. Abusorrah, K. Sedraoui, Decentralized bi-level stochastic optimization approach for multi-agent multi-energy networked micro-grids with multi-energy storage technologies, Energy 22 (2022), 123223, <https://doi.org/10.1016/j.energy.2022.123223>.
- [70] M.M. Gamil, T. Senju, H. Takahashi, A.M. Hemeida, N. Krishna, M.E. Lotfy, Optimal multi-objective sizing of a residential microgrid in Egypt with different ToU demand response percentages, Sustain. Cities Soc. 75 (2021), 103293, <https://doi.org/10.1016/j.scs.2021.103293>.
- [71] D. Zhang, S. Li, M. Sun, Z. O'Neill, An optimal and learning-based demand response and home energy management system, IEEE Trans. Smart Grid. 7 (4) (2016) 1790–1801, <https://doi.org/10.1109/TSG.2016.2552169>.
- [72] T.C. Chiu, Y.Y. Shih, A.C. Pang, C.W. Pai, Optimized day-ahead pricing with renewable energy demand-side management for smart grids, IEEE Internet Things J. 4 (2) (2016) 374–383, <https://doi.org/10.1109/JIOT.2016.2556006>.
- [73] P. Akbary, M. Ghiasi, M.R. Pourkheranjani, H. Alipour, N. Ghadimi, Extracting appropriate nodal marginal prices for all types of committed reserve, Comput. Econ. 53 (1) (2019) 1–26, <https://doi.org/10.1007/s10614-017-9716-2>.
- [74] R. Mulla, Hourly Energy Consumption: Over 10 years of hourly energy consumption data from PJM in Megawatts, Available: <https://www.kaggle.com/robikscube/hourly-energy-consumption>, 2018. (Accessed 27 May 2021).
- [75] Andrej, Solar Radiation Prediction: Task from NASA Hackathon, Available: <https://www.kaggle.com/dronio/SolarEnergy>, 2017. (Accessed 27 May 2021).
- [76] D. Beniaguev, Historical Hourly Weather Data 2012–2017, Available: <https://www.kaggle.com/selfishgene/historical-hourly-weather-data>, 2017. (Accessed 27 May 2021).
- [77] R. Lu, S.H. Hong, X. Zhang, A dynamic pricing demand response algorithm for smart grid: reinforcement learning approach, Appl. Energy 15 (220) (2018) 220–230, <https://doi.org/10.1016/j.apenergy.2018.03.072>.
- [78] M. Yu, S.H. Hong, Incentive-based demand response considering hierarchical electricity market: a Stackelberg game approach, Appl. Energy 1 (203) (2017) 267–279, <https://doi.org/10.1016/j.apenergy.2017.06.010>.
- [79] S. Li, B. Ke, Study of battery modeling using mathematical and circuit oriented approaches, in: 2011 IEEE Power and Energy Society General Meeting, IEEE, 2011, pp. 1–8, <https://doi.org/10.1109/PES.2011.6039230>.
- [80] D. Srivjan, R. Thogaru, A. Mitra, in: Energy Management in Grid Assisted BESS Integrated Solar PV Based Smart Charging Station. IECON 2019 - 45th Annu. Conf. IEEE Ind. Electron. Soc 2019, IEEE, 2019, pp. 6363–6368, <https://doi.org/10.1109/IECON.2019.8927767>.
- [81] W. Zhu, J. Guo, G. Zhao, B. Zeng, Optimal sizing of an island hybrid microgrid based on improved multi-objective Grey wolf optimizer, Processes 8 (2020) 1581, <https://doi.org/10.3390/pr8121581>.
- [82] Commonwealth Edison Company, Real-time and Day-ahead Hourly Price, Available: <https://hourlypricing.comed.com/live-prices/>, 2021. (Accessed 12 February 2021).
- [83] C. Christopher Columbus, S.P. Simon, Profit based unit commitment: a parallel ABC approach using a workstation cluster, Comput. Electr. Eng. 38 (2012) 724–745, <https://doi.org/10.1016/j.compeleceng.2011.09.002>.